

IMPERIAL

MENG INDIVIDUAL PROJECT

IMPERIAL COLLEGE LONDON

DEPARTMENT OF COMPUTING

Adversarial Robustness and Verification of Liquid Neural Networks for Time-Series Prediction

Author:

Viyana Raj

Supervisor:

Dr. Alessio Lomuscio

Second Marker:

Alyssa Renata

June 13, 2025

Abstract

The increasing deployment of neural networks in safety-critical dynamic systems (such as autonomous vehicles) has highlighted the need for formal guarantees of robustness, which quantify the model’s ability to maintain correct outputs under adversarial input perturbations. However, the verification of such properties becomes significantly more complex with Liquid Neural Networks, which are a novel class of time-continuous architectures that use ODEs to provide improved adaptability and robustness in sequential learning tasks. The project addresses this gap by conducting a comprehensive adversarial evaluation of LNNs, benchmarking their resilience on a 2D timeseries input against a range of adversarial attacks, which aim to perturb the input slightly and cause significant output errors, exposing vulnerabilities. A diverse set of adversarial attacks, ranging from gradient-based methods (like PGD and FGSM) to gradient-free time-manipulation methods, were employed to expose different failure modes and sensitivities across temporal models. In addition, a novel verification pipeline was implemented using interval bound propagation through the auto_LiRPA framework, producing verifiable bounds on prediction intervals. This enabled formal robustness certification of the LNN model behavior under l_∞ perturbations. Results demonstrate that, given comparable predictive performance to their discrete-time counterparts, LNNs’ continuous internal dynamics yield greater inherent resistance to adversarial manipulation. Under attack, they demonstrated lower empirical degradation than the comparative models. These findings reinforce the value of continuous-time and liquid neuron dynamics for building robust machine learning systems and provide a reproducible benchmark for future verification research in this domain.

Acknowledgements

I would like to express my sincere gratitude to my supervisor, Dr. Alessio Lomuscio, for his guidance, support, and encouragement throughout this project. I also thank Alyssa Renata, my second marker, for her insightful feedback. I am deeply grateful to my friends and family for their unwavering support during this research journey.

Contents

1	Introduction	5
1.1	Motivation	5
1.2	Contributions	5
2	Background and Literature Review	7
2.1	Liquid Neural Networks	7
2.2	Adversarial Attacks	11
2.3	Neural Network Verification	12
3	Liquid Neural Network Design and Implementation	15
3.1	Design Overview	15
3.2	Wiring and Connectivity	15
3.3	LTC Neuron Dynamics	16
3.4	Network Architecture	18
3.5	Training Configuration (and dataset)	19
3.6	Training Behaviour	20
4	Comparative Models	23
4.1	Introduction to Baseline Models	23
4.2	Temporal Convolutional Network (TCN)	23
4.3	Long Short-Term Memory Network (LSTM)	26
4.4	Transformer Model	28
5	Adversarial Attack Methodology and Robustness Certification	31
5.1	Introduction to Adversarial Attacks	31
5.2	Fast Gradient Sign Method (FGSM)	31
5.3	Projected Gradient Descent (PGD)	32
5.4	DeepFool-Inspired Directional Attack	33
5.5	Simultaneous Perturbation Stochastic Approximation (SPSA)	34
5.6	Time-Warping Attack	34
5.7	Continuous-Time Perturbation Attack	35
5.8	Summary of Attack Design and Implementation Decisions	36
5.9	Certified Robustness Analysis of the LNN via Interval Bound Propagation	37
6	Evaluation	40
6.1	Evaluation Metrics	40
6.2	Quantitative Results	41
6.3	Visual Analysis	42
6.4	Discussion of Results	49
6.5	Defences for Liquid Neural Networks	49
7	Conclusion	52
7.1	Summary of Work	52
7.2	Future Work	52

Chapter 1

Introduction

1.1 Motivation

In fields where system reliability is crucial, such as autonomous control, medical diagnostics, and financial forecasting, the susceptibility of machine learning models to adversarial inputs presents an important challenge. Even small, well-crafted perturbations can push high-performing neural networks to produce incorrect outputs. This raises concerns about their trustworthiness in real-world deployments.

Liquid Neural Networks (LNNs), which draw from the dynamics of continuous-time systems, offer a compact and adaptive alternative to more conventional architectures. This resemblance stems from their representation as parameterised ordinary differential equations (ODEs), allowing each neuron to evolve its state continuously over time. This closely mirrors the adaptive membrane dynamics observed in biological neurons. Whilst traditional neural networks such as LSTMs have been studied extensively under adversarial conditions, there is little existing work on how LNNs behave when subjected to such threats.

The goal is to rigorously evaluate the adversarial robustness of LNNs and compare their behaviour with other widely used sequential models (such as such as LSTMs, TCNs, and Transformers). By doing so, the project contributes to a better quantification of the benefits/vulnerabilities that the continuous-time formulation of LNNs offer, when exposed to adversarial manipulation.

1.2 Contributions

This report presents, to the best of our knowledge, the first in-depth adversarial analysis of Liquid Neural Networks. Whilst this analysis for models such as CNNs and LSTMs are somewhat mainstream, this is yet to be done for LNNs. The main contributions can be summarised as follows:

- An experimental framework for applying a broad range of adversarial attacks (including gradient-based, gradient-free, and temporal strategies) to four sequential architectures: LNN, LSTM, TCN, and Transformer.
- Custom implementations of continuous-time and time-warping attacks, specifically designed to exploit the state dynamics unique to ODE-based models like the LNN.
- A detailed comparative evaluation of adversarial responses using both quantitative metrics and visual trajectory analysis, highlighting failure patterns such as phase drift, memory corruption, and temporal smoothing effects.
- The use of certified robustness techniques via the `auto_LiRPA` library, allowing formal verification of LNN model stability under bounded perturbations.
- Aggregated robustness metrics are presented and analysed for interpretability. These include percentage degradation, output deviation, and local Lipschitz constants.

In addition to these contributions, this work provides a unified platform for evaluating the connection between model architecture and adversarial vulnerability in time-series prediction tasks. We focus on how

inductive biases shape a model’s response to different attack surfaces. These biases include recurrence, convolutional locality, attention-based context aggregation, and continuous-time dynamics. The findings offer insights into both the practical robustness of Liquid Neural Networks but also the broader question of how architectural choices influence adversarial behaviour in low-data, temporally sensitive settings.

Chapter 2

Background and Literature Review

In this chapter, we explore the current research on this topic. First, by exploring the theory behind liquid neural networks, in comparison to deep neural networks. Then, by investigating popular adversarial attack methods and assessing their suitability to liquid neural network structures. Finally, current verification methods are discussed, along with their suitability to liquid neural networks. The reader should have an understanding of (traditional) neural networks and linear algebra concepts.

2.1 Liquid Neural Networks

Liquid neural networks, introduced by Ramin Hasani et al. (2021) [1], are a novel class of AI algorithms, designed to maintain adaptability after completing training. These are inspired by the communication patterns of brain cells, which are flexible and responsive to new/unseen data even after their initial training phase.

Traditional neural networks use fixed architectures and static parameters, so require retraining to handle new information. Liquid neural networks use **continuous-time dynamics** to enable their state to evolve smoothly over time. This means they can dynamically adjust their responses to changing inputs during inference. This structure allows these networks to be robust against perturbations and capable of generating complex behaviors without requiring large-scale architectures.

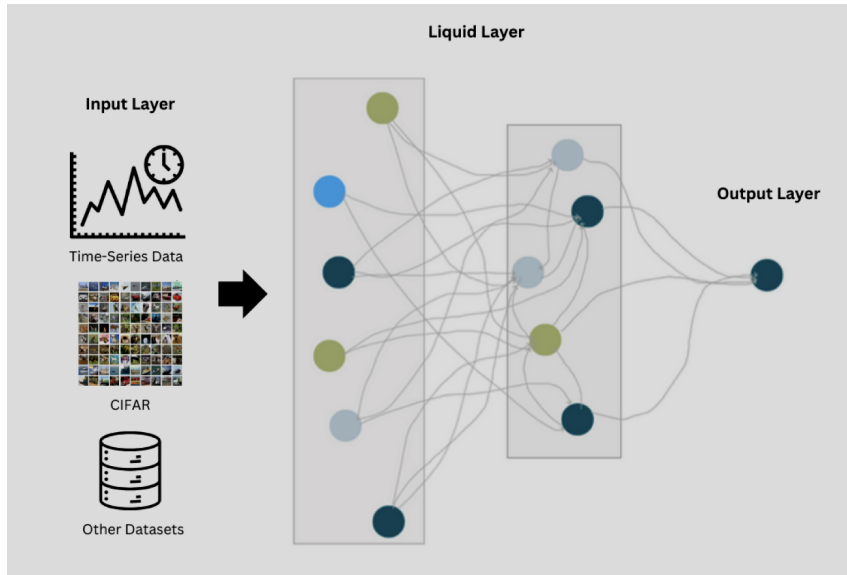


Figure 2.1: Schematic Diagram of a Liquid Neural Network [2]. Figure illustrates the simplified architecture of an LNN, starting with the input layer receiving time-series data. The data then flows into the liquid layer, where dynamic, non-linear processing occurs through a complex network of interconnected neurons. Finally, the processed information is relayed to the output layer.

LNNs use differential equations to simulate the continuous/dynamic processing and plasticity of the brain. Since LNN neurons communicate selectively with a subset of other neurons, connections formed are sparse (unlike traditional deep neural networks with dense fully-connected layers). This makes LNNs more computationally efficient than deep neural networks.

There are a range of applications of LNNs. Hasani suggests that their inherent adaptability makes them suitable for tasks requiring real-time learning and decision-making, such as autonomous driving and medical diagnosis. Their efficiency could address several challenges associated with large-scale machine learning systems, including issues related to interpretability, accountability, and environmental impact due to high carbon footprints. [3]

Continuous-Time Dynamical Systems/Differential Equations

A **continuous-time dynamical system** is a mathematical model used to describe a system that evolves over time in a way that is continuous (rather than discrete). This means the state of the system changes smoothly as a function of time, without abrupt jumps.

In the context of liquid neural networks, the neurons' states evolve as continuous-time dynamical systems. Each neuron's state is governed by **differential equations**, enabling the network to process information dynamically and adaptively, much like physical systems in the real world. This is inspired by biological neurons, where the activity of each neuron is influenced dynamically by inputs and changes over time.

The state of each neuron $x_i(t)$ in an LNN evolves over time according to a differential equation, expressed as:

$$\frac{dx_i(t)}{dt} = f(x_i(t), u_i(t), t; \theta_i), \quad (2.1)$$

where:

- $x_i(t)$: The internal state of the i -th neuron at time t ,
- $u_i(t)$: The input signal to the i -th neuron at time t ,
- t : Time, treated as a continuous variable,
- θ_i : Trainable parameters of the neuron, such as weights and biases,
- $f(\cdot)$: A function (usually nonlinear) describing the neuron's dynamics.

A common differential equation is the **leaky integrator dynamics**, where the state evolves as:

$$\frac{dx_i(t)}{dt} = -\alpha x_i(t) + \sum_{j=1}^N w_{ij} h(x_j(t)) + u_i(t),$$

with:

- $-\alpha x_i(t)$: A "leakage" term causing the neuron's state to decay over time, with $\alpha > 0$ representing the decay rate (temporal decay),
- $\sum_{j=1}^N w_{ij} h(x_j(t))$: The weighted input from other neurons, where w_{ij} is the weight from neuron j to i , and $h(x_j(t))$ is a nonlinear activation function (e.g., tanh or ReLU),
- $u_i(t)$: An external input signal.

For more complex systems, **nonlinear terms** can be included, resulting in equations such as:

$$\frac{dx_i(t)}{dt} = g(x_i(t)) + \sum_{j=1}^N w_{ij} \sigma(x_j(t)) + u_i(t),$$

where $g(x_i(t))$ models intrinsic nonlinear dynamics, and $\sigma(x_j(t))$ is a nonlinear activation function.

A liquid neural network, as a continuous-time dynamical system, has several important features. First, it ensures **smooth evolution**, where the neuron states evolve continuously over time according to differential equations. This smooth state transition is essential for modeling time-dependent values in tasks like

time-series forecasting or control systems. In addition, the dynamics of the network incorporate **time dependency** t explicitly or depend solely on the current state $x(t)$, enabling the network to capture both static and dynamic temporal relationships. Liquid neural networks are also typically **deterministic**, with their future states fully defined by the current states and inputs, but they can also accommodate **stochastic elements** to model uncertainty or noise in the environment. Finally, the network may operate under **linear** dynamics, such as $f(x) = Ax + Bu$, which are efficient but limited in complexity, or **nonlinear** dynamics, like $f(x) = \tanh(Wx + b)$, which allow the network to represent intricate patterns and adaptive behaviours.

LNN Training

During training, the above differential equations (2.1) define how each neurons processes information. For each labelled training data sample, the following process occurs.

During the **forward pass**, the system of differential equations is numerically solved over time, starting from an initial state $x(0)$. Inputs $u(t)$ and parameters θ_i drive the evolution of neuron states $x_i(t)$.

The network then outputs a value, derived from the neuron states. This is compared to the target output to compute a **loss function**.

During **backpropagation through time**, gradients of the loss with respect to trainable parameters (θ_i) are computed by differentiating through the differential equations using methods like automatic differentiation or adjoint sensitivity analysis.

Finally, **optimization algorithms** (e.g. gradient descent) update the parameters of the DEs to minimize the loss.

LNN Inference

During inference, the same differential equations govern the neuron states, but parameters (θ_i) are fixed. The network processes dynamic inputs $u(t)$ in real-time. The equation also considers the neuron's previous state $x_i(t)$, which is dependent on previous input values $u(t)$. Thus, the output of each neuron is dependent on the parameters, current input values, and previously seen input values.

Advantages of LNNs

Using differential equations in LNNs provides several advantages.

Temporal Modelling

Continuous dynamics are well-suited for time-dependent tasks. This means LNNs can be used to find time-based relationships in data (temporal modeling). This form of 'memory' is highly beneficial in time-series tasks.

The nonlinear nature of $f(x_i(t))$ ensures that the network captures complex temporal dependencies, allowing it to adjust its behavior based on the sequence and timing of inputs. This dynamic capability provides the network with a form of memory, enabling it to adapt to new scenarios even outside the training set.

This is in contrast to static models which consider data points to be independent and identically distributed.

Adaptability

Dynamic state evolution allows the network to adapt during deployment.

The differential equation model (2.1) for liquid neural networks allows for state evolution even after training, resulting in increased adaptability. This is achieved by the continuous dynamics governing neuron states, which enable the network to respond dynamically to real-time inputs and changing environments.

In the DE model, $x_i(t)$ is the state of the i -th neuron at time t , $u_i(t)$ represents external inputs, t is time, and θ_i are trainable parameters (e.g., weights and biases). After training, the parameters θ_i are fixed, but the neuron states $x_i(t)$ continue to respond dynamically to new inputs $u_i(t)$. This means the network

integrates real-time inputs into its state over time, adapting its behavior dynamically to variations in the input patterns or the timing of events.

The differential equations governing the states ensure that even small variations in the input influence the system, enabling real-time adaptation.

This provides several advantages. LNNs excel in real-world scenarios involving dynamic environments, such as robotics [4] and control systems.

For example, an LNN controlling a robotic arm in a dynamic environment would learn general principles of motion and control during training. During inference, as new obstacles appear or external forces are applied, the network integrates this new information into its state $x_i(t)$ dynamically. This allows the robotic arm to adjust its movements in real time without needing retraining for each specific scenario.

In addition, by dynamically evolving its states, the network generalizes better to unseen data patterns by interpolating between learned behaviors.

Efficiency

Liquid neural networks (LNNs) are inherently more efficient than traditional deep neural networks (DNNs) due to their ability to maintain sparser representations. At any given time, only a subset of an LNNs' neurons or parameters are significantly active or contribute to the system's computations. This sparsity reduces the computational overhead while retaining the network's performance and adaptability.

This is because continuous-time dynamics favor selective activity. In LNNs, neuron states evolved continuously over time, according to the differential equation 2.1. Here $f(\cdot)$ determines how each neuron state changes based on its inputs, past states, and parameters. The use of continuous-time dynamics enables neurons to become active only when relevant input signals $u_i(t)$ or temporal events trigger them. This selective activity leads to fewer neurons being active at a given time, resulting in sparse representations.

LNNs are designed to work efficiently with fewer parameters compared to DNNs. While in traditional DNNs, layers are often densely connected, meaning all neurons in one layer interact with all neurons in the next layer. LNNs use sparse connectivity patterns, where neurons only interact with a limited subset of other neurons. This reflects real-world systems, such as biological brains, where neurons form selective, sparse connections. The sparsity of connections reduces the number of computations required during both training and inference.

LNNs allow the internal states of neurons to evolve over time and depend on the dynamics of the inputs. Because of this adaptability, only neurons relevant to the current input remain active. This reduces unnecessary computations and avoids the inefficiencies of global activation in traditional DNNs.

The continuous dynamics of LNNs inherently encode temporal dependencies. Unlike recurrent neural networks (RNNs) or deep learning models that require explicit mechanisms like memory gates (e.g., in LSTMs or GRUs), LNNs rely on the fluid evolution of neuron states. This reduces the overhead of managing and updating memory states, further contributing to sparsity and efficiency.

The sparse nature of LNNs offers several advantages over traditional DNNs, including reduced computational cost (minimizing matrix operations), lower energy consumption, better scalability, and robustness to overfitting (as sparse connectivity can act as a regularization mechanism by ensuring only essential features are focussed on).

Stability

LNNs exhibit greater stability and robustness to noise compared to traditional DNNs.

Continuous time dynamics and differential equations encode stability constraints, ensuring smooth transitions between states.

In LNNs, the state of each neuron evolves over time according to the differential equation 2.1. The continuous nature of these equations ensures that the neuron states change gradually over time. As a result, sudden spikes in the input $u_i(t)$ (caused by noise) are naturally smoothed out. This gradual evolution prevents abrupt changes in the neuron states, making the network less sensitive to transient noise.

In addition, neuron states evolve in response to both the current input $u_i(t)$ and past states $x_i(t)$. This integration over time allows the network to prioritize long-term patterns in the input and ignore temporary noise. The feedback from past states enables temporal filtering, where only meaningful input changes accumulate and influence the network’s output. In contrast, the layer-by-layer static activations in DNNs make them more susceptible to noise.

In traditional DNNs, noisy inputs can propagate through the network, often being amplified by dense connections and static parameter updates. To avoid this, special techniques can be used such as dropout. However, LNNs achieve this implicitly, by using sparse and selective connections. This limits the propagation of noise across the network. The continuous evolution of states ensures that transient noise does not significantly affect downstream neurons or outputs.

This enhanced stability has a range of benefits. LNNs perform well in real-world settings where inputs are often corrupted. The intrinsic smoothing abilities of LNNs also reduces the amount of noise-filtering preprocessing required.

2.2 Adversarial Attacks

Adversarial robustness has become a central concern in the deployment of deep learning models, particularly for safety-critical systems. Foundational studies in this area, such as those by Szegedy et al. [5] and Goodfellow et al. [6], demonstrated that small, human-imperceptible perturbations can cause significant model mispredictions.

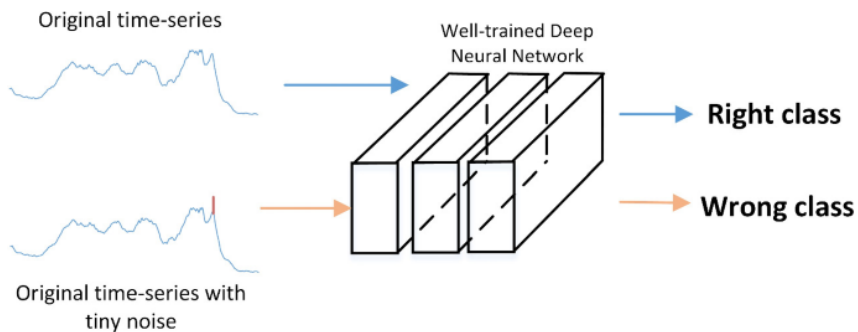


Figure 2.2: Adversarial Attack on a timeseries input [7] [7]

This motivated the development of a range of attack strategies, most notably gradient-based methods like the Fast Gradient Sign Method (FGSM) [6], its iterative counterpart PGD [8], and more geometry-aware attacks such as DeepFool [9]. In scenarios where gradient access is limited or unavailable, black-box attacks like Simultaneous Perturbation Stochastic Approximation (SPSA) [10] have proven effective.

These attack strategies have been extensively studied across various architectures including Convolutional Neural Networks (CNNs), Recurrent Neural Networks (RNNs), and Transformer-based models. Recent literature has also explored temporal robustness in sequence prediction tasks, particularly in domains such as speech [11], motion tracking [12], and control systems [13].

While LNNs have demonstrated strong performance on control and robotic benchmarks, their robustness under adversarial conditions remains largely unexplored.

This project represents the first systematic exploration of adversarial vulnerabilities in Liquid Neural Networks. We evaluate the vulnerability of LNNs under a range of attack regimes, including FGSM, PGD, SPSA, and DeepFool-like variants, as well as trajectory-specific perturbations such as time-warping and continuous-time adversarial noise. While these attacks have been previously tested on discrete models like LSTMs and TCNs [14], their effects on the internal ODE solvers and state dynamics of LNNs are not well understood.

By adapting these methods to the continuous setting of LNNs and comparing the outcomes to conventional temporal models, this work provides new insights into the failure modes, dynamic vulnerabilities, and potential robustness benefits of biologically-inspired time-continuous architectures under adversarial threat.

2.3 Neural Network Verification

In this section we explore the problem of neural network verification. We look at current methods used for DNN verification, which will form the inspiration for a liquid neural network verification approach. The suitability of these to LNNs must be evaluated.

The Verification Problem

Verification problems can involve concrete bounds on the input and linear programming (LP) constraints on the output. Formally, the problem can be defined as follows:

Definition 2.2.1.1 Let $f : \mathbb{R}^n \rightarrow \mathbb{R}^m$ be a neural network, and let $\mathcal{X} = \{x' \in \mathbb{R}^n \mid x_i^l \leq x'_i \leq x_i^u\}$ represent the set of valid inputs constrained by the lower and upper bounds x^l, x^u . Given a set of linear constraints on the output ψ_y , let $\mathcal{Y} = \{y \mid \psi_y\}$ denote the set of outputs satisfying ψ_y . The verification problem is to determine whether $x' \in \mathcal{X} \implies f(x') \in \mathcal{Y}$, or to find a counterexample $x' \in \mathcal{X}$ such that this implication is not true.

For input and output constraints as defined above, the goal is either to prove that no valid input violates the output constraints or to find an input that does. If no input satisfies the output constraints, we declare the property as “safe.” Otherwise, if such an input exists, the property is deemed “unsafe,” and the corresponding input serves as a counterexample. [15]

Motivation

Verification of neural networks is a crucial problem, especially when a new architecture (such as liquid neural networks) is being researched. This is because neural networks are often deployed in safety-critical applications, such as autonomous vehicles or medical diagnosis, where unpredictability can cause significant harm. Neural networks are also vulnerable to adversarial attacks, which is when small perturbations within input data (often unnoticeable to the human eye) cause significant undesired changes in the output. This vulnerability poses a serious threat to their reliability and trustworthiness. Verification ensures that the network behaves as expected under specified conditions, whilst robustness verification focuses on guaranteeing that small perturbations in the input do not lead to misclassifications or unsafe behavior. By formally proving properties of neural networks or identifying counterexamples, verification helps to ensure safety and mitigate risks in real-world deployments.

Symbolic and Interval Propagation Methods

This section explores methods that focus on propagating bounds through liquid neural networks, which verifies their robustness when faced with input perturbations. **Symbolic Interval Propagation (SIP)** is a technique that computes conservative output bounds using interval arithmetic, providing a computationally efficient way to check for robustness. **CROWN (Certified Robustness to Weight Perturbations)** is more complex, and introduces linear approximations which improves the precision of robustness verification.

SIP (Symbolic Interval Propagation)

SIP is a scalable and efficient technique for verifying liquid neural networks by propagating symbolic intervals through the layers of the network to bound the range of possible outputs. For LNNs governed by neural ODEs with the equation 2.1, SIP can be applied to discretize and propagate bounds over time, handling non-linearity and ensuring robustness and safety properties are satisfied under perturbations.

Steps in SIP:

1. **Input Interval Initialization:** Define the input range as intervals $[l_i, u_i]$ for each dimension x_i , forming a hyper-rectangle. These intervals are represented symbolically to maintain dependencies between variables.
2. **Symbolic Propagation Through Layers:** At each discretized time step or layer:
 - **Affine Transformations:** For a layer $z = Wx + b$, bounds are propagated symbolically:

$$l_z = W \cdot l_x + b, \quad u_z = W \cdot u_x + b.$$

- **Nonlinear Activations:** Nonlinearities like ReLU or tanh are handled by updating bounds:

$$\text{ReLU: } [\max(0, l_z), \max(0, u_z)], \quad \text{Tanh: } [\tanh(l_z), \tanh(u_z)].$$

3. **Output Interval Verification:** The final output intervals are compared against safety or robustness properties. For example, given input perturbations δx , the output bounds $F(x)$ must satisfy:

$$F(x + \delta x) \subseteq [F_L, F_U],$$

where F_L and F_U are symbolic bounds on the output.

Advantages for Liquid Neural Networks SIP is well-suited for LNNs due to its ability to handle the continuous evolution of states in neural ODEs:

- Precision: Symbolic intervals maintain variable dependencies, producing tighter bounds than traditional interval arithmetic.
- Efficiency: Propagation avoids the computational cost of exact methods, making SIP scalable for larger networks.
- Adaptability: SIP can handle nonlinear dynamics in LNNs through accurate approximations of activation functions.

Practical Considerations One consideration is over-approximation - accumulated conservativeness may reduce precision in deeper networks. Also, complex nonlinearities (within highly nonlinear layers such as softmax) require additional approximations, introducing potential conservatism. Finally, for neural ODEs, time discretization must balance accuracy with computational cost.

CROWN (Certified Robustness to Weight Perturbations)

CROWN (Certified Robustness to Weight Perturbations) [16] is a general framework for certifying the robustness of neural networks, including those with non-linear activation functions. It achieves this by bounding the outputs of the network using adaptive linear (or quadratic) upper and lower bounds for each activation function. For liquid neural networks, governed by neural ODEs, CROWN can be adapted to certify robustness by discretizing the continuous dynamics and applying its bounding technique to each time step.

CROWN provides an efficient and scalable method for verifying the robustness of LNNs. The propagated adapted bounds ensure that perturbations in the input do not lead to significant deviations in the output.

Mathematical Framework Consider a liquid neural network modeled as:

$$\frac{dx(t)}{dt} = f(x(t), t, \theta),$$

where $x(t) \in \mathbb{R}^n$ is the state, $f(x, t, \theta)$ describes the dynamics, and θ represents the parameters. For a given perturbed input $x_0 \in \mathbb{R}^n$ within an ℓ_p -ball:

$$x \in B_p(x_0, \epsilon) = \{x \mid \|x - x_0\|_p \leq \epsilon\},$$

CROWN aims to compute certified bounds $F_L(x) \leq F(x) \leq F_U(x)$, where $F(x)$ is the output of the neural ODE after a fixed time horizon T .

Bounding Nonlinearities For each activation function $\sigma(y)$, CROWN constructs linear upper and lower bounds:

$$h_U(y) = \alpha_U y + \beta_U, \quad h_L(y) = \alpha_L y + \beta_L,$$

such that $h_L(y) \leq \sigma(y) \leq h_U(y)$ over a pre-activation range $[l, u]$. These bounds are propagated through the layers of the network. For LNNs, this involves discretizing the time domain into intervals $[t_k, t_{k+1}]$ and applying the bounds iteratively at each time step.

Output Certification To certify robustness, CROWN computes bounds on the network's output $F(x)$. Using the layer-by-layer propagation of the upper and lower bounds, the output bounds are expressed as:

$$F_U(x) = \Lambda^{(0)}x + \sum_{k=1}^m \Lambda^{(k)}(b^{(k)} + \Delta^{(k)}), \quad F_L(x) = \Omega^{(0)}x + \sum_{k=1}^m \Omega^{(k)}(b^{(k)} + \Theta^{(k)}),$$

where Λ and Ω are matrices representing the upper and lower bound propagation, and Δ and Θ account for biases introduced by non-linearities.

Application to Neural ODEs For neural ODEs, the propagation framework is adapted to account for the continuous evolution of states. The bounds are computed at each discretized step t_k , ensuring that the dynamics satisfy the robustness conditions:

$$F_U(x_0) - F_L(x_0) \geq \delta,$$

where δ is the minimum required margin for robustness.

Practical Implementation CROWN can be implemented as follows:

1. **Define Input Bounds:** Specify the ℓ_p -ball around the input x_0 and initialize the pre-activation bounds for the first layer.
2. **Propagate Bounds:** Compute the upper and lower bounds layer-by-layer using the adaptive linear approximations.
3. **Certify Robustness:** Verify that the certified bounds at the output satisfy the desired robustness property (e.g., consistent classification).

Chapter 3

Liquid Neural Network Design and Implementation

3.1 Design Overview

This chapter outlines the implementation of the Liquid Neural Network (LNN) developed in PyTorch for sequential 2D time-series prediction. The architecture is based on the Liquid Time-Constant (LTC) neuron model, which simulates continuous-time dynamics through ordinary differential equations (ODEs) and shows properties of neural adaptability and temporal memory.

The aim of the implementation was to create a biologically-inspired, interpretable recurrent model with competitive performance on trajectory prediction tasks. Unlike conventional RNNs or LSTMs, the LNN is governed by time-continuous equations rather than discrete updates, providing finer control over neuronal dynamics.

The following principles guided the design:

- **Framework:** PyTorch was selected due to its flexible dynamic graph construction and ease of integrating custom layers with automatic differentiation.
- **Neuron Dynamics:** The neuron model was designed to emulate leaky integrate-and-fire (LIF) behaviour with added plasticity through modulated reversal potentials and conductances.
- **Time Unfolding:** Each forward pass of the LNN integrates over multiple internal time steps (ODE unfolds) to approximate the continuous-time solution, reflecting membrane voltage evolution.
- **Baseline Comparison:** To benchmark performance, identical training and evaluation protocols were implemented for alternative architectures (LSTM, TCN) using the same data.

The implementation was adapted from an incomplete and partially functional tutorial model [17], which, despite containing bugs and missing components, provided a useful structural foundation for further development and refinement.

The following sections document the architecture, neuron formulation, wiring strategy, training setup, and performance characteristics of the LNN.

3.2 Wiring and Connectivity

LNNs have a sparse and biologically motivated connectivity structure. To simulate the non-uniform and random nature of synaptic wiring observed in biological networks, a custom class named `RandomWiring` was implemented.

This class generates two adjacency matrices:

- A **recurrent adjacency matrix** of shape $(n \times n)$ defining internal connections between neurons within the hidden layer.

- A **sensory adjacency matrix** of shape $(d_{\text{in}} \times n)$ which defines the input-to-hidden connectivity.

Each matrix contains continuous values sampled from a uniform distribution on $[0, 1]$, which are later used to create binary masks or to modulate weight strengths.

The `RandomWiring` class also generates reversal potentials: `erev` for neuron-neuron connections, and `sensory_erev` for input-synapse connections. These potentials are initialised from a uniform range $[-0.2, 0.2]$ and are treated as fixed, non-learnable parameters.

The use of fixed sparse masks in the class emulate the limited number of active connections in real cortical microcircuits, enabling **biological plausibility**. In addition, each **randomised instantiation** of `RandomWiring` results in a different network topology, allowing stochastic variation in experiments.

Finally, the sensory and recurrent wiring are **decoupled**, to enable the model to explicitly distinguish between input-driven and internal dynamic behaviour.

Below is a simplified example of the `RandomWiring` class:

```

1  class RandomWiring:
2      def __init__(self, input_dim, output_dim, neuron_count):
3          self.adjacency_matrix = np.random.uniform(0, 1, (neuron_count,
4              neuron_count))
5          self.sensory_adjacency_matrix = np.random.uniform(0, 1, (input_dim,
6              neuron_count))
7
8      def erev_initializer(self):
9          return np.random.uniform(-0.2, 0.2, (neuron_count, neuron_count))
10
11     def sensory_erev_initializer(self):
12         return np.random.uniform(-0.2, 0.2, (input_dim, neuron_count))

```

Listing 3.1: Simplified RandomWiring class

3.3 LTC Neuron Dynamics

The core unit of the LNN is the `LIFNeuronLayer`, a custom PyTorch module that simulates the behaviour of leaky integrate-and-fire neurons (also known as liquid time-constant neurons). These neurons operate using a continuous-time dynamical model controlled by a first-order differential equation, capturing the evolution of membrane potentials in response to internal and external stimuli.

The model integrates over time using a discretised ODE solver implemented within the forward pass. Specifically, it unfolds the membrane update equation over a fixed number of steps (`ode_unfolds`) using an Euler-like method [1].

The update rule is determined by the equation:

$$\begin{aligned}
v_i^{(t+1)} &= \frac{1}{Z} \left(\mathcal{S}(c_{m,i}) \cdot v_i^{(t)} + \mathcal{S}(g_{\text{leak},i}) \cdot V_{\text{leak},i} \right. \\
&\quad + \sum_j \underbrace{\mathcal{S}(w_{ij}) \cdot \sigma(v_j^{(t)}; \mu_{ij}, \sigma_{ij}) \cdot E_{\text{rev},ij}}_{\text{Recurrent synaptic current}} \\
&\quad \left. + \sum_k \underbrace{\mathcal{S}(w_{ki}^{\text{sens}}) \cdot \sigma(x_k; \mu_{ki}^{\text{sens}}, \sigma_{ki}^{\text{sens}}) \cdot E_{\text{rev},ki}^{\text{sens}}}_{\text{Sensory synaptic current}} \right) \tag{3.1}
\end{aligned}$$

$$Z = \mathcal{S}(c_{m,i}) + \mathcal{S}(g_{\text{leak},i}) + \sum_j \mathcal{S}(w_{ij}) \cdot \sigma(v_j^{(t)}; \mu_{ij}, \sigma_{ij}) + \sum_k \mathcal{S}(w_{ki}^{\text{sens}}) \cdot \sigma(x_k; \mu_{ki}^{\text{sens}}, \sigma_{ki}^{\text{sens}}) + \varepsilon \tag{3.2}$$

where:

- $\mathcal{S}(\cdot) = \text{Softplus}(\cdot) = \log(1 + e^{(\cdot)})$: nonlinearity ensuring positivity of weights and conductances
- $v_i^{(t)}$: membrane potential of neuron i at ODE step t
- x_k : sensory input from dimension k
- $\sigma(v; \mu, \sigma) = \text{sigmoid}(\sigma(v - \mu))$: synaptic activation function
- w_{ij} : weight from neuron j to neuron i (recurrent)
- w_{ki}^{sens} : weight from input k to neuron i (sensory)
- μ, σ : learnable sigmoid parameters (mean and scale)
- $E_{\text{rev}}, E_{\text{rev}}^{\text{sens}}$: synaptic reversal potentials
- V_{leak} : fixed leak reversal potential
- c_m, g_{leak} : learnable membrane capacitance and leak conductance
- ε : small constant for numerical stability

This formulation reflects the true internal update logic of the `LIFNeuronLayer` implementation, where each neuron's potential evolves through a biophysically inspired ODE governed by input-specific and recurrent dynamics.

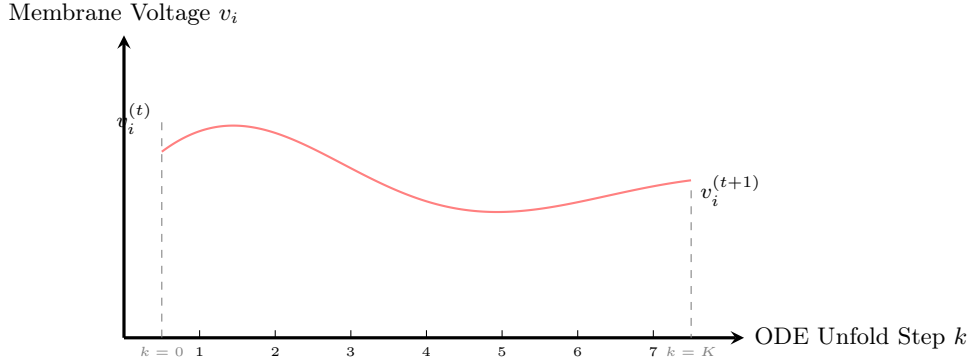


Figure 3.1: Example internal membrane voltage trace across K ODE unfolding steps for a single neuron. This entire graph represents the internal dynamics used to compute $v_i^{(t+1)}$ from $v_i^{(t)}$, in a single timestep.

Unlike traditional RNNs or LSTMs, which update their hidden state in a single discrete operation per time step, Liquid Time-Constant neurons simulate fine-grained membrane voltage dynamics by performing multiple internal updates within each input timestep. This behaviour is governed by the discretised solution of the differential equations (see Equation 3.1 and Equation 3.2).

At each unfolding step, the membrane potential is updated using a softplus-modulated combination of capacitive memory, leak current, and synaptic input currents. These updates reflect physical dynamics such as charging, leak, and synaptic integration, enabling the neuron to adaptively integrate information over sub-timestep resolution. The final membrane voltage $v_i^{(t+1)}$ is the result of this integration process and is passed forward in time.

This is different from gated memory in LSTMs, which uses learnable gates and affine transformations, or temporal convolutions in TCNs, which apply fixed receptive filters. Instead, the LTC neuron learns dynamic temporal behaviour through time constants and nonlinear integration, making it particularly suited to tasks that require fine temporal resolution and state-dependent transitions.

Implementation Details:

- **Learnable Parameters:** All biophysical constants (capacitance, leak conductance, reversal potentials, synaptic weights) are learnable, providing flexibility in dynamic behaviour.
- **Softplus Regularisation:** Weights and conductances are passed through `Softplus` to enforce positivity while allowing gradients to flow smoothly during training.

- **ODE Unfolding:** The number of internal solver steps is fixed (`ode_unfolds` = 12) to balance numerical precision with computational cost.
- **Sparsity Masks:** Both recurrent and sensory activations are element-wise masked using the adjacency matrices from `RandomWiring`, enforcing fixed sparsity throughout training.

Below is the ODE solver implementation within the `LIFNeuronLayer` class:

```

1 def ode_solver(self, inputs, state, elapsed_time):
2     v_pre = state
3     for _ in range(self.ode_unfolds):
4         synaptic_input = compute_synaptic_activation(v_pre)
5         numerator = self.cm * v_pre + self.gleak * self.vleak + synaptic_input
6         denominator = self.cm + self.gleak + synaptic_conductance
7         v_pre = numerator / (denominator + self.epsilon)
8     return v_pre

```

Listing 3.2: Simplified LTC neuron forward method

This allows neurons to respond to both present input and also to their internal temporal dynamics, mimicking continuous-time memory traces observed in biological neurons.

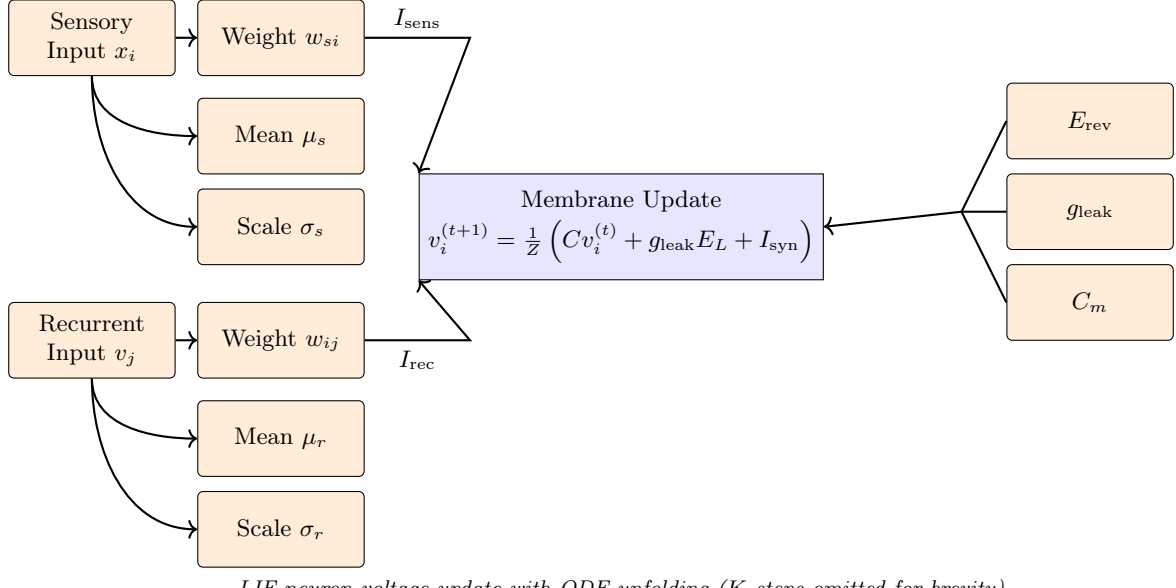


Figure 3.2: Internal structure of a single LIF neuron used in the Liquid Time-Constant Network. Inputs undergo non-linear transformations based on trainable μ and σ , and the resulting activations are integrated using biophysical parameters (leak conductance g_{leak} , membrane capacitance C_m , and reversal potentials E_{rev}).

3.4 Network Architecture

The full LNN is constructed by embedding the LTC neuron layer inside a recurrent wrapper, implemented as a custom `LTCRNN` module. This wrapper sequentially passes each time step of the input through the same `LIFNeuronLayer`, maintaining a hidden state that evolves over time. The resulting structure can be viewed as a biologically grounded alternative to traditional RNN cells.

The architecture accepts an input tensor of shape (B, T, d_{in}) , where B is the batch size, T is the sequence length, and d_{in} is the input dimension (two in this case, corresponding to 2D spatial coordinates). For each time step t , the neuron layer receives the t -th slice of the sequence and updates the hidden state, generating a predicted output of shape (B, T, d_{out}) .

Design Considerations

While designing the LTCRNN architecture, there were several key design decisions made. The hidden state dimensionality (i.e. number of LTC neurons) defined the model capacity; lower values reduce overfitting risk and improve computational efficiency at the cost of limited expressiveness. In addition, the voltage traces themselves are treated as predictions instead of applying a separate output layer. This means membrane state is directly used as a continuous output signal. To maximise efficiency (and GPU parallelism) of tensor operations during training/inference, all sequences are processed in batch-major form (following PyTorch convention).

Below is a simplified version of this architecture:

```

1  class LTCRNN(nn.Module):
2      def __init__(self, wiring, input_dim, hidden_dim, output_dim):
3          self.cell = LIFNeuronLayer(wiring)
4          ...
5
6      def forward(self, inputs):
7          batch_size, seq_len, _ = inputs.size()
8          states = torch.zeros(batch_size, self.hidden_dim)
9          outputs = []
10         for t in range(seq_len):
11             out, states = self.cell(inputs[:, t, :], states)
12             outputs.append(out)
13         return torch.stack(outputs, dim=1)

```

Listing 3.3: Structure of the LTCRNN module

The design maintains a clear distinction between the continuous-time neuronal dynamics and the sequence-level integration logic. Thus, it is both modular and biologically interpretable, and compatible with standardised modern deep learning tools.

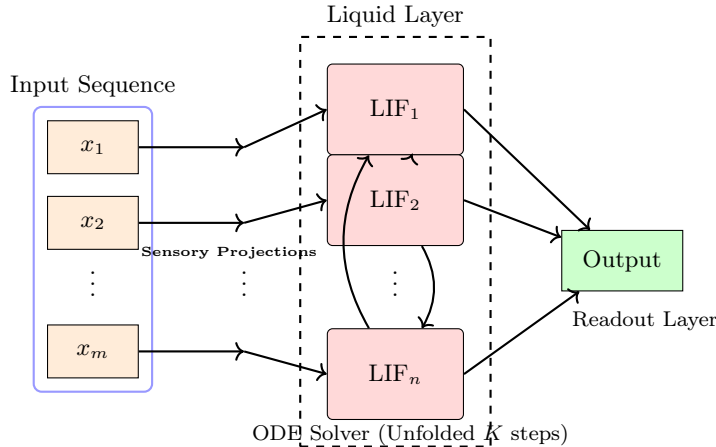


Figure 3.3: Architecture of the Liquid Time-Constant Network (LNN). Inputs project through learned sensory filters to a sparsely recurrent Liquid Layer of LIF neurons. Dynamics are integrated using an internal ODE solver with unfolding. Final outputs are read from a low-dimensional projection.

3.5 Training Configuration (and dataset)

The LNN was trained on a synthetic 2D spiral trajectory dataset, chosen for its smooth temporal structure and nonlinearity. Each data point consists of an (x, y) coordinate, and the model's aim is to predict the next point in the sequence (given a fixed-length input window). The 'sequential' nature of the task makes it well-suited for testing temporal memory and continuous dynamics.

The synthetically-generated dataset ensured control over noise and resolution, which allowed clearer attribution of error sources to model limitations rather than data irregularities.

A supervised learning approach was used; inputs and targets were created by shifting a sliding window of length $T = 3$ over the full spiral. The small sequence length was chosen to reduce training complexity while still allowing temporal dependencies to be captured. Each input sequence of three time steps was paired with the corresponding next three steps as the target output.

The dataset was split into training and validation sets, with the training set containing 80% of the data and the validation set containing 20%. This split was randomised to ensure that the model generalised well to unseen data.

Data Preprocessing

- All inputs were standardised using the training set mean and standard deviation.
- Targets were normalised in the same way to preserve scale consistency.
- The spiral dataset was generated programmatically with adjustable number of points and turns.

Training Parameters Mean Squared Error (`nn.MSELoss()`) was used to penalise deviations from the ground truth trajectory. Adam was chosen as the optimiser due to its fast convergence and robustness to parameter scaling, with a learning rate of 0.005. The model was trained for 2000 epochs, with periodic visual evaluation every 100 epochs. Input sequences were split into overlapping windows and grouped into batches of size 32, allowing efficient GPU utilisation while preserving temporal continuity. A random 80/20 train-validation split was applied, with shuffling to prevent memorisation of input order.

Below is the training process implementation:

```

1  for epoch in range(num_epochs):
2      lnn_model.train()
3      total_loss = 0
4      for x_batch, y_batch in zip(input_batches, target_batches):
5          optimizer.zero_grad()
6          outputs = lnn_model(x_batch)
7          loss = criterion(outputs, y_batch)
8          loss.backward()
9          optimizer.step()
10         total_loss += loss.item()

```

Listing 3.4: Simplified training loop for the LNN

The training loop includes evaluation checkpoints where predicted trajectories are plotted and compared to ground truth. These visualisations provided insights into convergence behaviour, beyond scalar loss values.

3.6 Training Behaviour

Throughout training, model performance was monitored both quantitatively (via validation loss) and qualitatively (through trajectory plots), every 100 epochs.

The main trends observed during training were:

- Loss decreased steadily in early epochs, with diminishing returns as training progressed.
- In some cases, small fluctuations in validation loss were observed, likely due to the non-convexity of the parameter landscape and the biological variability induced by random wiring.
- Visual predictions of the trajectory showed clear improvement over time. Early predictions were coarse approximations, while later epochs gave smoother and more accurate predictions.

Trajectory Loss Curves

To evaluate the model's learning progress and generalisation, we record the full-sequence mean squared error (MSE) first on the entire spiral sequence (which contains the training datapoints and the held-out validation datapoints), and then on a separate unseen evaluation spiral, at each epoch. Rather than

separately plotting training and validation loss — which are contiguous segments of the same spiral trajectory, they are treated as a single sequence. This is because temporal continuity is essential in modelling dynamical systems. This avoids misleading interpretations that might arise from artificial segmentation of a naturally evolving system.

The following plots illustrates training and validation behaviour over time (the second is zoomed to highlight differences between the training/validation spiral and evaluation spiral):

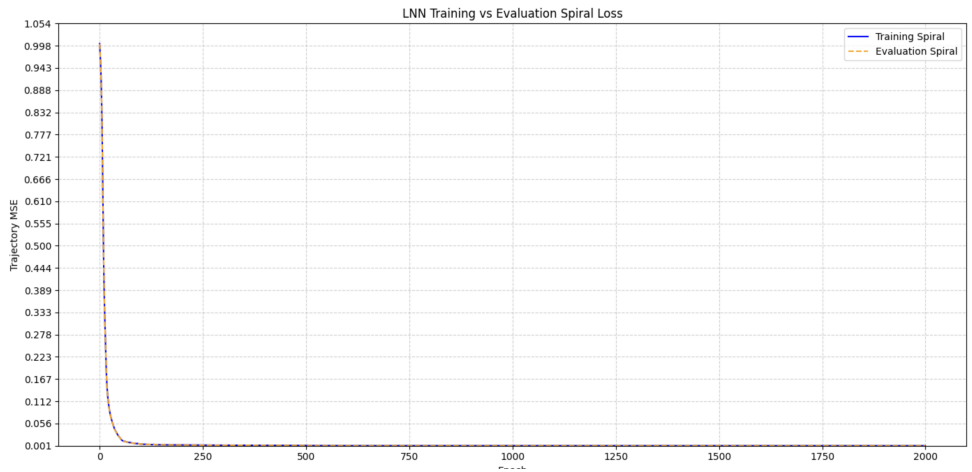


Figure 3.4: Training and validation loss over epochs.

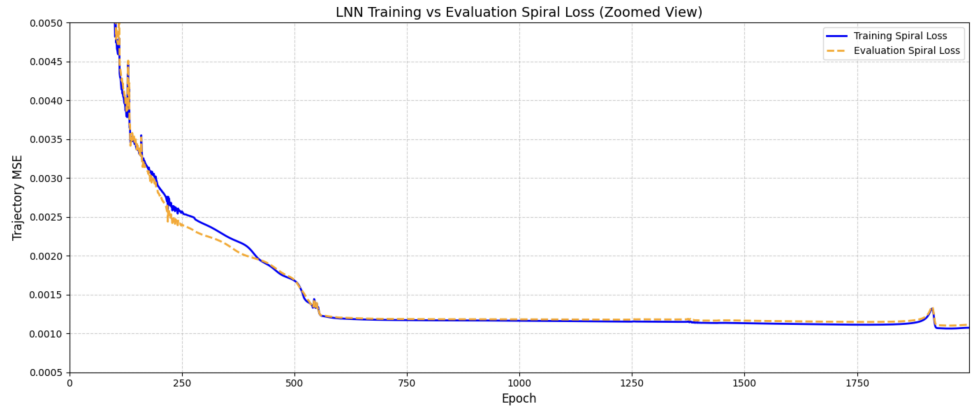


Figure 3.5: Training and validation loss over epochs (zoomed).

Early in training, both curves decrease rapidly, suggesting that the model learns the underlying structure efficiently. As training proceeds, the two curves converge, with the evaluation spiral maintaining a slightly higher loss, indicating some generalisation gap but also demonstrating stable extrapolation beyond the training path. Importantly, neither curve exhibits significant divergence or overfitting behaviour, which supports the robustness and consistency of the trained model.

Qualitative Evaluation

Visually, the predicted path over time showed that the LNN was able to maintain smooth curvature and approximate the rotational dynamics of the spiral without overshooting or excessive lag. This was true even on validation data not seen during training.

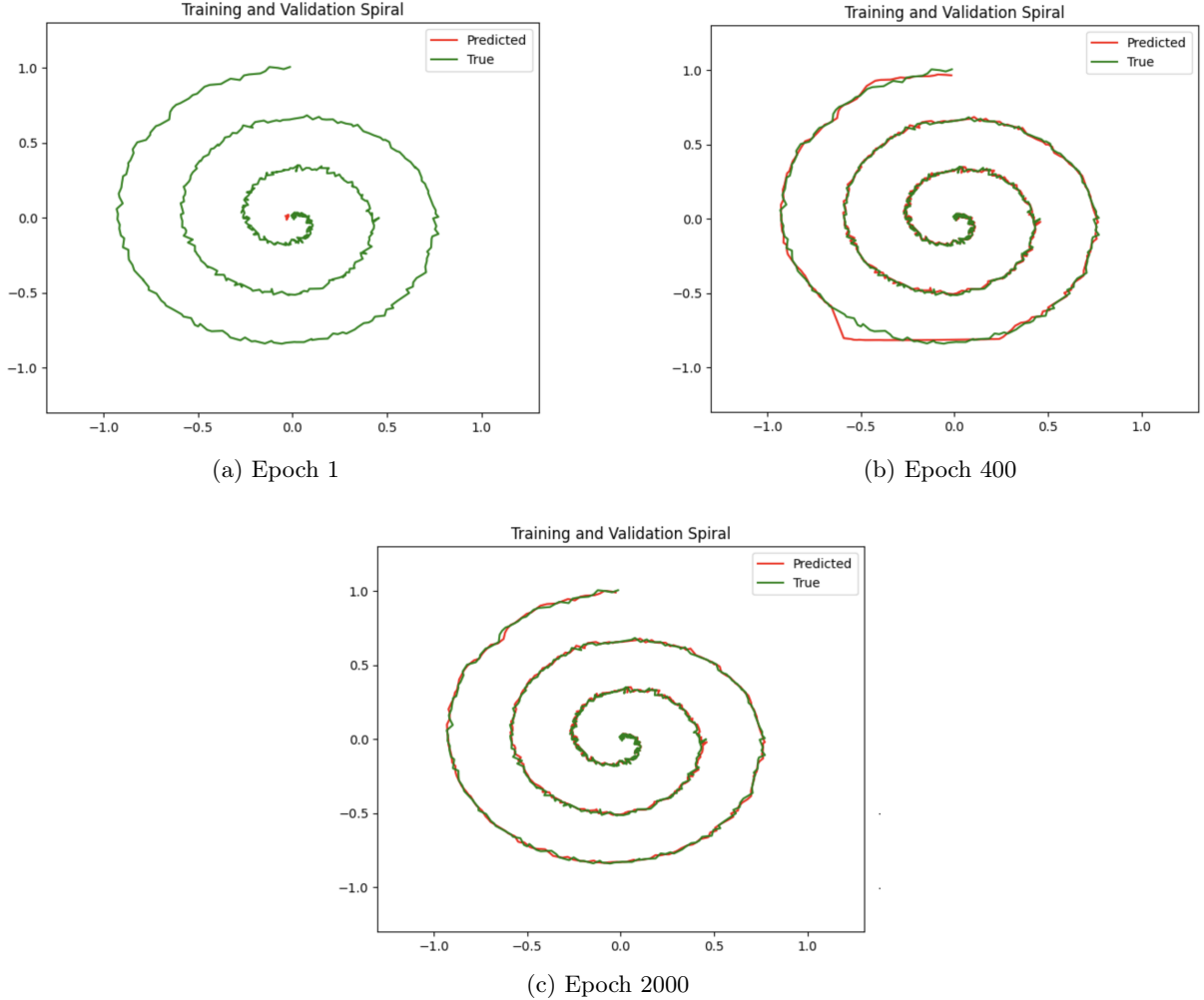


Figure 3.6: LLN predicted vs true spiral trajectories across training: early, mid, and final epochs (denormalised training and validation spiral)

Observed Patterns Across Training Runs

The number of internal steps in the membrane integration process (**ODE unfolding depth**) contributed significantly to trajectory stability. Deeper unfolding improved smoothness, but with diminishing returns. The architectures' fixed wiring helped constrain overfitting and contributed to better generalisation than a fully connected architecture. Notably, runs with different initialisations showed **performance variations** in loss curves and convergence speed, indicating sensitivity to initial wiring or parameter seeds.

Despite simpler architectures having shorter training times (e.g. LSTMs), LLN's had superior interpretability and stability in capturing the underlying continuous structure of the problem.

Although trained on fixed-length input windows, models were evaluated on full-sequence inference without autoregressive rollouts. This mismatch is empirically validated to yield stable and accurate predictions on smooth trajectories.

Chapter 4

Comparative Models

4.1 Introduction to Baseline Models

To provide context for the robustness and verification of the Liquid Neural Network (LNN), we benchmark its performance against three established neural architectures: the Temporal Convolutional Network (TCN), the Long Short-Term Memory (LSTM) network, and the Transformer model. All models are trained on the same trajectory prediction task, using identical datasets, normalisation, loss functions, and training schedules as the LNN.

The selection of these baselines is motivated by their contrasting inductive biases and proven success in modelling sequential data. The LSTM is a recurrent architecture that introduces gating mechanisms and persistent internal states, enabling it to model long-range temporal dependencies through iterative state updates. The TCN, however, uses on dilated causal convolutions and fixed temporal receptive fields, making it structurally different from recurrent networks and well-suited for parallel computation. The transformer model is an attention-based architecture, which eliminates recurrence altogether, and dynamically weight input positions using self-attention mechanisms. It applies positional encodings to retain order information.

Each model is carefully designed and trained to have similar loss and accuracy (details of which can be found in evaluation 6). This allows for fair comparison of robustness.

By evaluating the behaviour of these models under clean and adversarial conditions, we aim to identify both their predictive accuracy, and their robustness, sensitivity to perturbation, and qualitative output characteristics. These insights provide context for assessing the LNN in the following aspects:

- **Temporal memory:** How effectively each model retains and processes sequential dependencies
- **Structural robustness:** The influence of architectural constraints on noise sensitivity
- **Gradient stability:** The relationship between loss geometry and adversarial vulnerability

4.2 Temporal Convolutional Network (TCN)

Overview and Motivation

The TCN is a fully convolutional architecture designed for sequential data. Unlike RNN-based models, which process inputs recursively and maintain an internal hidden state, TCNs rely on 1D convolutions applied over the temporal axis. This allows for parallel computation and more stable gradients, particularly for long sequences.

TCN's use **dilated convolutions**, which expand the receptive field exponentially with depth while preserving causality. This makes them highly effective at modelling long-range dependencies without the vanishing gradient issues that often affect RNNs.

Theoretical Background

For a 1D input sequence $x \in \mathbb{R}^{T \times d}$, a dilated convolution with kernel k and dilation factor d is defined as:

$$(y *_d k)(t) = \sum_{i=0}^{k-1} k(i) \cdot x(t - d \cdot i)$$

This structure allows the model to observe wider contexts with fewer parameters and layers.

In practice, the TCN is constructed using **residual blocks** with stacked dilated convolutions, dropout, and skip connections to stabilise training. Zero-padding is used to ensure output length matches input length.

Model Architecture

The implemented TCN consists of 3 residual blocks, each with: two dilated 1D convolutional layers with kernel size 3, ReLU activations and dropout regularisation, and optional 1x1 convolutions for matching input-output dimensions. Each residual block has a dilation rate of 1, 2, and 4 respectively (exponentially increasing dilation).

An output convolution maps the final hidden representation to the desired 2D coordinate space.

Below is a simplified example of the TCN model implementation:

```

1  class ResidualBlock(nn.Module):
2      def __init__(self, in_channels, out_channels, kernel_size, dilation, dropout):
3          ...
4          self.conv1 = nn.Conv1d(..., dilation=dilation)
5          self.conv2 = nn.Conv1d(..., dilation=dilation)
6
7  class TCN(nn.Module):
8      def __init__(self, input_dim=2, hidden_channels=128, ...):
9          self.tcn = nn.Sequential(*residual_blocks)
10         self.output_layer = nn.Conv1d(hidden_channels, output_dim, 1)

```

Listing 4.1: Simplified TCN architecture

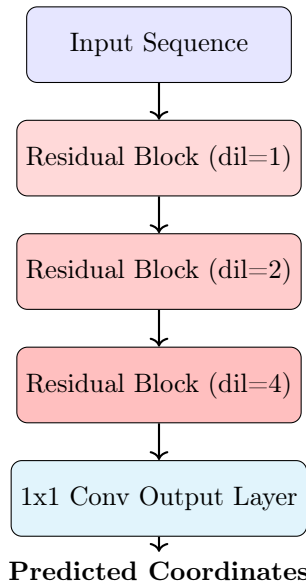


Figure 4.1: Temporal Convolutional Network (TCN) architecture

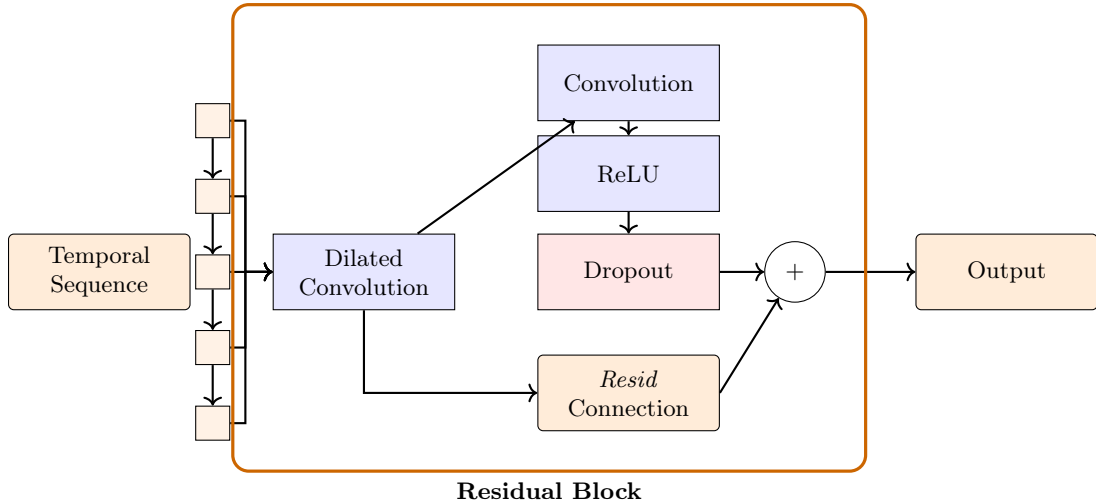


Figure 4.2: Structure of a TCN Residual Block. Each convolution uses dilation to increase receptive field, while residual skip connections and dropout stabilise training.

Training Configuration

The TCN was trained on the same spiral dataset as the LNN, with identical batch size, learning rate, loss function (Smooth L1), and normalisation pipeline. The model was optimised using Adam and a learning rate scheduler that halved the rate every 500 steps.

Performance and Behaviour

The TCN demonstrated strong performance on the trajectory prediction task, converging more quickly than the LNN and producing smooth outputs even with a small receptive field. The use of dilated convolutions allowed the model to predict coordinated curvature without explicitly tracking hidden state over time.

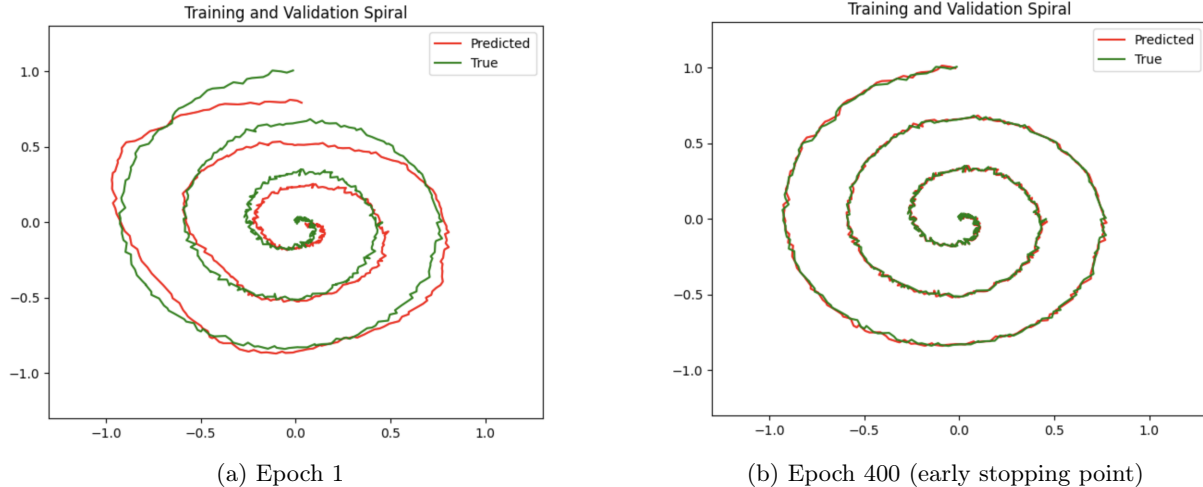


Figure 4.3: TCN predicted vs true spiral trajectories across training: early and final epochs (denormalised training and validation spiral)

Design Considerations

- **Causality:** All convolutions were causal, ensuring no future information was used during prediction.
- **Parameter efficiency:** Despite having no recurrence, the TCN was able to model complex spirals with relatively few layers and a small parameter set.

- **Regularisation:** Dropout was used within each block to avoid overfitting (since convolutional models tend to memorise local structures in small datasets).

Despite lacking the dynamic time constants of the LNN, the TCN proved to be a strong baseline in terms of speed, stability, and accuracy under clean conditions.

4.3 Long Short-Term Memory Network (LSTM)

Overview and Motivation

The LSTM network is a popular recurrent neural architectures for sequential learning tasks. It was introduced to address the limitations of classical RNNs, particularly the vanishing and exploding gradient problems during backpropagation through time. The LSTM uses gated memory units that regulate the flow of information over time.

LSTMs have the ability to retain past information via internal cell states. This makes them well-suited for temporal tasks, such as trajectory prediction.

LSTM Cell Mechanics

An LSTM cell maintains two internal states: a hidden state h_t and a cell state c_t . The cell's behaviour is controlled by three gates:

$$\begin{aligned} f_t &= \sigma(W_f x_t + U_f h_{t-1} + b_f) && \text{(forget gate)} \\ i_t &= \sigma(W_i x_t + U_i h_{t-1} + b_i) && \text{(input gate)} \\ o_t &= \sigma(W_o x_t + U_o h_{t-1} + b_o) && \text{(output gate)} \\ \tilde{c}_t &= \tanh(W_c x_t + U_c h_{t-1} + b_c) && \text{(cell candidate)} \\ c_t &= f_t \odot c_{t-1} + i_t \odot \tilde{c}_t \\ h_t &= o_t \odot \tanh(c_t) \end{aligned}$$

These equations define how the LSTM updates its memory and hidden representations at each time step. W_* and U_* are learnable weight matrices applied to the current input x_t and previous hidden state h_{t-1} respectively; b_* are bias vectors. Each subscript * corresponds to a particular gate (f : forget, i : input, o : output, c : cell candidate). \odot denotes elementwise multiplication.

Model Implementation

The LSTM was implemented using PyTorch's built-in `nn.LSTM` module. A two-layer LSTM was used, with 128 hidden units per layer. The final hidden state was passed through a linear projection layer to output a 2D coordinate.

```

1 class LSTMModel(nn.Module):
2     def __init__(self, input_dim=2, hidden_dim=128, num_layers=2, output_dim=2):
3         self.lstm = nn.LSTM(input_dim, hidden_dim, num_layers, batch_first=True)
4         self.output_layer = nn.Linear(hidden_dim, output_dim)
5
6     def forward(self, x):
7         out, _ = self.lstm(x)
8         return self.output_layer(out)

```

Listing 4.2: Simplified LSTM model structure

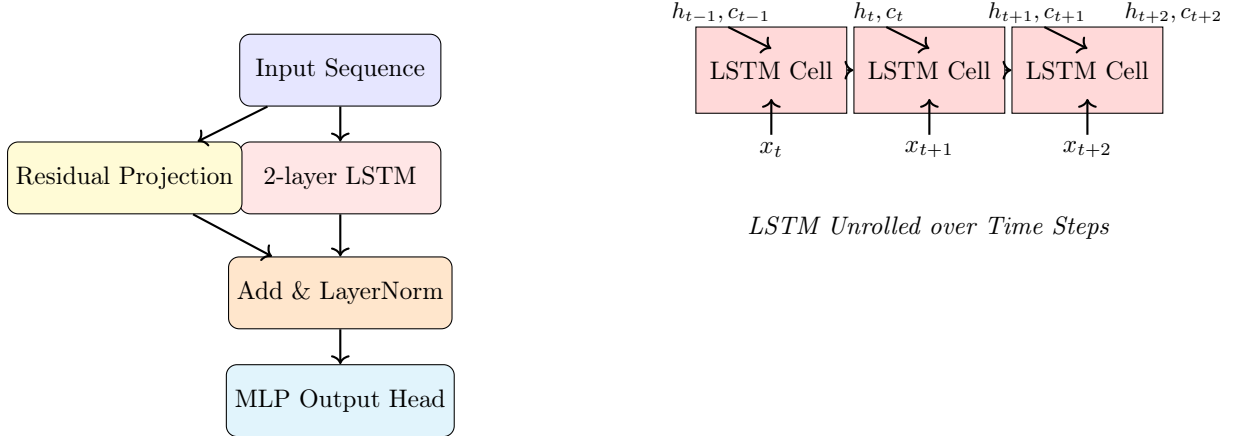


Figure 4.4: Architecture of the LSTM model. The left shows residual-enhanced flow through a 2-layer LSTM, while the right shows the LSTM unrolled across time with hidden and cell state transitions.

Training Configuration

The LSTM was trained using the same dataset and preprocessing pipeline as the LNN and TCN. The Smooth L1 loss was used, and training was performed over 1000 epochs with a learning rate of 0.005. A step decay scheduler was applied halfway through training.

Training Observations

The LSTM showed stable training behaviour and low final validation loss. However, unlike the TCN and LNN, it exhibited slightly slower convergence. Its outputs were smooth and consistent, although it occasionally underfit regions with sharper curvature.

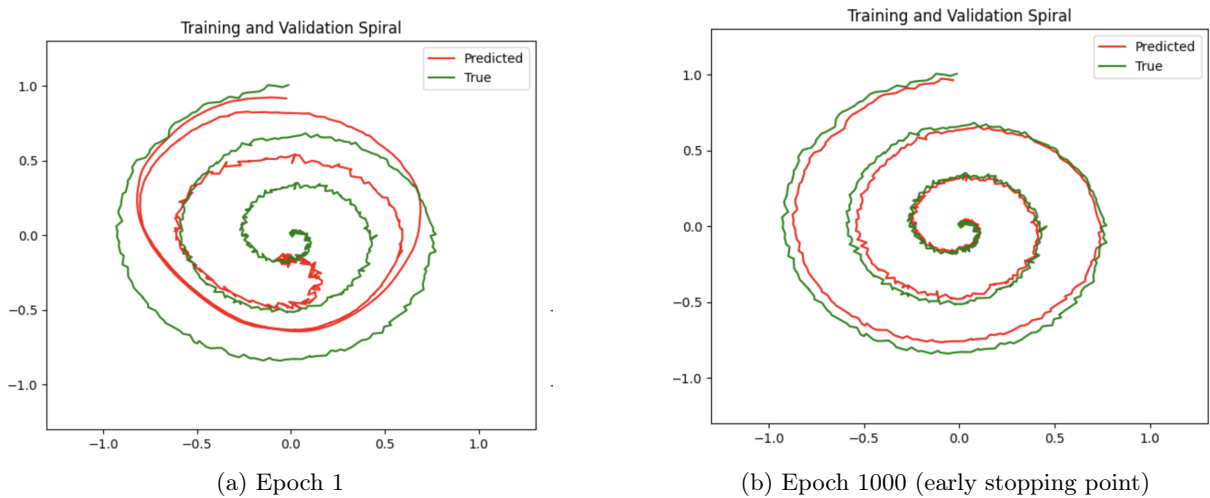


Figure 4.5: LSTM predicted vs true spiral trajectories across training: early and final epochs (denormalised training and validation spiral)

While the LSTM offers a reliable baseline for temporal prediction, its recurrent structure can make it more sensitive to gradient-based perturbations.

4.4 Transformer Model

Overview and Motivation

The Transformer is an attention-based architecture originally developed for sequence transduction tasks in NLP. The Transformer architecture implemented in this project is a lightweight variant of the original Transformer encoder proposed by Vaswani et al. [18], adapted for short-length continuous 2D time-series data. Unlike recurrent or convolutional models, the Transformer uses **self-attention** to learn dependencies across the input sequence in parallel. This decouples sequence processing from sequential computation and provides greater flexibility in learning temporal relationships.

Transformer Encoder Design

The main aspect of the model is the **Transformer encoder**, a stack of layers built around self-attention and feedforward submodules. Each encoder layer learns to transform the input sequence into a more abstract representation by allowing each token (timestep) to attend to others, subject to a causal constraint.

Each encoder layer consists of the following components:

- **Multi-Head Self-Attention:** The model uses four attention heads, each projecting the input into different subspaces. For an input sequence $X \in \mathbb{R}^{T \times d}$, the self-attention mechanism computes:

$$\text{Attention}(Q, K, V) = \text{softmax}\left(\frac{QK^\top}{\sqrt{d}} + M\right)V$$

where Q , K , and V are learned linear projections of the input, and M is a **causal mask**: a triangular matrix filled with $-\infty$ above the diagonal to prevent attention to future positions.

- **Feedforward Network:** Following attention, a two-layer feedforward block applies a non-linear transformation independently at each position:

$$\text{FFN}(x) = \text{GELU}(xW_1 + b_1)W_2 + b_2$$

with an intermediate hidden size of 256 and GELU activation, chosen for its smooth gradient properties.

- **Residual Connections and Layer Normalisation:** Both the attention and feedforward submodules are wrapped in residual connections and followed by **LayerNorm**, ensuring stable training and gradient propagation even across deep encoder stacks:

$$\text{LayerNorm}(x + \text{SubLayer}(x))$$

- **Dropout:** Dropout is applied to both the attention weights and the feedforward layers with a rate of 0.1, providing regularisation and improving generalisation on small datasets.

Two of these encoder layers are stacked, allowing the model to build hierarchical abstractions over the input sequence.

The transformer encoder processes input sequences in parallel, whilst still capturing autoregressive temporal dependencies via the attention mask. The resulting sequence of contextualised embeddings is then passed to a prediction head that maps each timestep to its corresponding 2D coordinate output.

Positional information is injected via **learnable positional embeddings**, which are added to the input projections before encoding. A **causal mask** is applied to ensure predictions at time t do not access future values (enforcing temporal directionality).

Model Architecture

The Transformer model used contains: an input projection layer mapping 2D inputs to a 128-dimensional latent space, two Transformer encoder layers, a causal attention mask (to enforce autoregressive prediction), and a residual MLP head that maps the encoder output back into 2D coordinates.

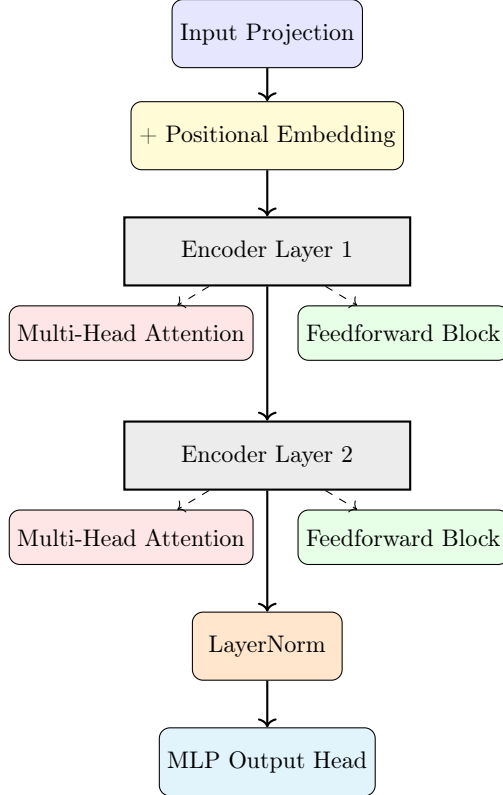


Figure 4.6: Architecture of the Transformer encoder used

Suitability for the Task

Despite the short sequence length (`seq_len = 3`), the transformer architecture is well-suited to this task for several reasons. Transformers allow for parallel processing of all timesteps, which improves training speed/efficiency. The model is also effective at capturing long-range dependencies in the dataset (despite short sequence length), since self-attention generalises well to higher-resolution datasets (longer sequences). In addition, the learnable positional embeddings allow the model to gain positional awareness without recurrence. This means the model can adaptively distinguish temporally adjacent inputs, enabling it to focus on the most informative timesteps. This helps to reduce sensitivity to noise and input distortions.

```

1 class TransformerModel(nn.Module):
2     def __init__(self, input_dim=2, model_dim=128, ...):
3         self.input_proj = nn.Linear(input_dim, model_dim)
4         self.encoder = nn.TransformerEncoder(...)
5         self.output_head = nn.Sequential(
6             nn.Linear(model_dim, model_dim // 2),
7             nn.ReLU(),
8             nn.Linear(model_dim // 2, output_dim)
9         )

```

Listing 4.3: Simplified Transformer architecture

Training Configuration

The Transformer was trained on the same spiral dataset as other baselines, using identical input pre-processing and normalisation. Optimisation was performed using AdamW with cosine annealing, and Smooth L1 loss was used as the objective. The model received short input sequences (length 3), and positional embeddings were learned from scratch.

Performance and Behaviour

Although the Transformer initially showed promising performance, with early convergence to low validation loss, extended training often led to **overfitting**, increasing loss and reduced trajectory fidelity. Its attention-based mechanism enabled flexibility but also made it sensitive to noise and hyperparameters, particularly given the small training context.

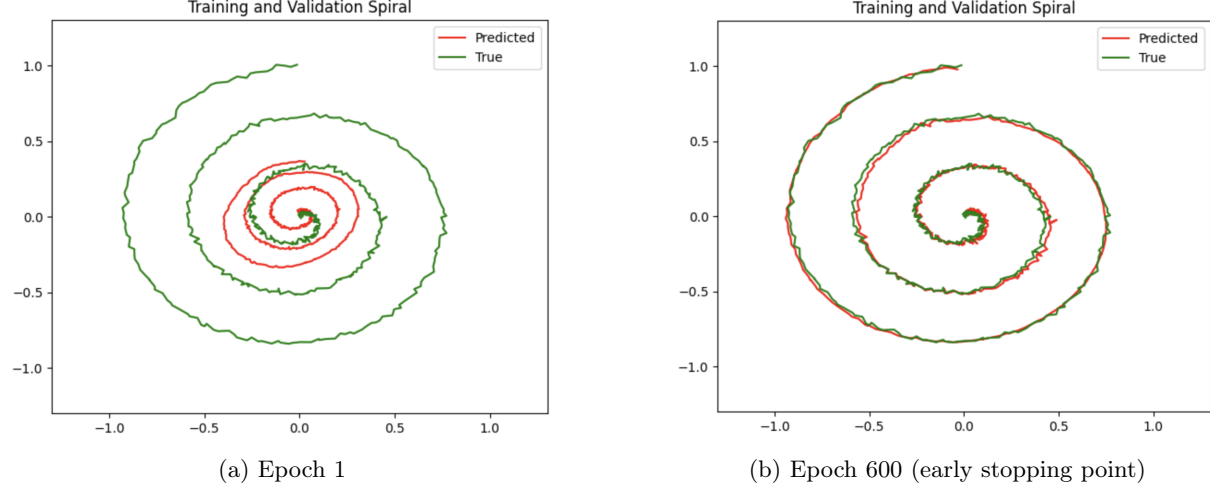


Figure 4.7: Transformer predicted vs true spiral trajectories across training: early and final epochs (denormalised training and validation spiral)

The Transformer model provides a powerful and flexible alternative to recurrent and convolutional architectures. However, its high capacity and limited structural bias made it more susceptible to generalisation issues (overfitting) under the noisy spiral task compared to more structured models like the TCN or LSTM. This highlights a trade-off between expressivity and inductive bias when data is limited.

Chapter 5

Adversarial Attack Methodology and Robustness Certification

5.1 Introduction to Adversarial Attacks

Adversarial attacks are deliberately constructed perturbations to input data that cause an ML model to make incorrect predictions with high confidence. These perturbations are often imperceptible or bounded in norm, but can expose vulnerabilities in the model's internal representations and loss surface geometry.

For sequential models such as the LNN, TCN, and LSTM, adversarial robustness is important, especially in safety-critical applications involving temporal dynamics. Several attacks are implemented in this project, targeting both gradient-accessible and gradient-free contexts, and include both white-box and black-box variants.

Each attack was evaluated under the same conditions, using:

- A fixed perturbation budget ϵ .
- Normalised data inputs, with identical initial conditions across models.
- Denormalised outputs for interpretability and comparison.

The metrics used for evaluating adversarial degradation included **Degradation Ratio**, **Deviation**, and **Local Sensitivity** (Lipschitz constant). For all models/attacks, further explanation of these metrics, numerical results, and qualitative analysis can be found in the evaluation section 6.

5.2 Fast Gradient Sign Method (FGSM)

The Fast Gradient Sign Method (FGSM) is a single-step adversarial attack first introduced by Goodfellow et al.[19] in 2014. It exploits the local linearity of neural networks by using the gradient of the loss function with respect to the input to perturb the input data in the direction that maximally increases loss.

Mathematical Representation

Given a model f_θ , a loss function $\mathcal{L}(f_\theta(x), y)$, and a clean input-target pair (x, y) , the FGSM adversarial input is constructed as:

$$x^{\text{adv}} = x + \epsilon \cdot \text{sign}(\nabla_x \mathcal{L}(f_\theta(x), y))$$

where ϵ controls the perturbation magnitude and $\text{sign}(\cdot)$ is applied elementwise. The method requires only a single forward and backward pass.

This adversarial input is then passed to the model, which produces an adversarial output that is examined.

Implementation Details

FGSM is implemented in this project using PyTorch's autograd engine. The input tensor is marked with `requires_grad=True` and gradients are computed by backpropagating through the MSE loss between model output and the clean target sequence. The sign of the gradient is scaled by ϵ and added to the input.

```

1 loss = F.mse_loss(model(x), y)
2 loss.backward()
3 perturbation = epsilon * x.grad.sign()
4 x_adv = x + perturbation

```

Listing 5.1: FGSM adversarial attack implementation

Attack Design Reflection:

FGSM is efficient but limited, as it assumes linearity and is easy to defend against with basic regularisation, so was used as a baseline attack method.

5.3 Projected Gradient Descent (PGD)

The PGD attack is an iterative extension of FGSM and is regarded as one of the stronger first-order adversaries in adversarial machine learning. Proposed by Madry et al. [8], PGD performs multiple small steps of perturbation in the direction of the loss gradient, updating the input to increase model error. After each step, the perturbed input is projected back onto an ℓ_p ball of fixed radius ϵ centered around the original input. The ℓ_p ball defines the set of allowable perturbations under a given norm constraint. For instance, the ℓ_∞ ball constrains each individual input dimension to change by no more than ϵ , and the ℓ_2 ball bounds the overall Euclidean distance of the perturbation. This constraint ensures that the adversarial input remains imperceptibly close to the original, preserving its semantics and attempting to fool the model.

Mathematical Representation

Given an input x and perturbation budget ϵ , PGD initializes the adversarial input as $x_0^{\text{adv}} = x + \delta$ (with δ small or random), and iteratively updates it as follows:

$$x_{t+1}^{\text{adv}} = \Pi_{B_\epsilon(x)}(x_t^{\text{adv}} + \alpha \cdot \text{sign}(\nabla_x \mathcal{L}(f_\theta(x_t^{\text{adv}}), y)))$$

Here, $\Pi_{B_\epsilon(x)}$ denotes the projection onto the ℓ_∞ ball centered at x with radius ϵ , and α is the step size.

Implementation Details

The attack was implemented using a fixed number of iterations (10). In each step, the model first performed a forward pass on the current adversarial input. Then, the loss was computed and backpropagated to obtain input gradients. Finally the adversarial input was updated using the signed gradient and clipped back to the ϵ -bounded domain. This process is then repeated, using the new adversarial input as the starting point.

```

1 for _ in range(num_iter):
2     output = model(x_adv)
3     loss = F.mse_loss(output, target)
4     loss.backward()
5     with torch.no_grad():
6         x_adv += alpha * x_adv.grad.sign()
7         perturbation = torch.clamp(x_adv - x_orig, min=-epsilon, max=epsilon)
8         x_adv = torch.clamp(x_orig + perturbation, min, max).detach().
            requires_grad_()

```

Listing 5.2: PGD Attack Loop (Simplified)

Design Choices

- **Step size α :** Set as 0.01 after empirical tuning to balance convergence and perturbation spread.
- **Projection radius ϵ :** Fixed at 0.05 to match FGSM budget for fair comparison.
- **Clipping bounds:** Enforced to retain normalised input range and ensure comparability with clean evaluations.

Unlike FGSM, PGD exposes high-curvature regions of the loss surface. The extent to which a model resists PGD steps provided insight into the local geometry of its input-output mapping.

5.4 DeepFool-Inspired Directional Attack

FGSM and PGD rely on sign-based or norm-bounded perturbations and, whilst effective, can be inefficient in identifying the minimal perturbation required for misprediction. DeepFool, introduced by Moosavi-Dezfooli et al. [?], aims to iteratively approximate the closest decision boundary in input space. Since it was originally designed for classification, a novel modified version was implemented here to exploit the gradient direction of loss for regression.

Mathematical Representation

In its original form, DeepFool linearises the classifier around the current point and computes the minimal step in the direction of the gradient that crosses the decision boundary. In the adaptation for regression, the perturbation is applied directly in the normalised direction of the loss gradient, without projection.

The update rule is given by:

$$x^{\text{adv}} = x + \eta \cdot \frac{\nabla_x \mathcal{L}(f(x), y)}{\|\nabla_x \mathcal{L}(f(x), y)\|_2 + \delta}$$

where η is a scalar perturbation magnitude and δ is a small stabilisation term to prevent division by zero.

Implementation Summary

The attack was implemented using a single or few iterations, computing the raw gradient of the loss with respect to the input and stepping along the normalised direction. Unlike PGD, no projection or clipping was applied. This was chosen to explore worst-case directional drift.

```

1 loss = F.mse_loss(model(x), y)
2 loss.backward()
3 gradient = x.grad.data
4 perturbation = eta * gradient / (torch.norm(gradient) + epsilon)
5 x_adv = x + perturbation

```

Listing 5.3: Directional (DeepFool-like) Gradient Attack

Design Considerations

- **Normalisation:** The gradient was normalised using ℓ_2 norm rather than using the sign, to emulate the boundary-seeking nature of DeepFool.
- **No projection:** This allowed the perturbation to fully reflect the underlying geometry of the loss surface, rather than artificially constraining it.
- **Step size tuning:** η was selected via a sweep, typically in the range [0.01, 0.05].

This attack highlights structural vulnerability that simpler norm-bounded methods could have missed. For continuous dynamics models like the LNN, sensitivity to gradient direction (rather than just amplitude) was observed.

5.5 Simultaneous Perturbation Stochastic Approximation (SPSA)

The Simultaneous Perturbation Stochastic Approximation (SPSA) attack is a gradient-free adversarial method designed for scenarios where gradient information is inaccessible, unreliable, or expensive to compute. Originally proposed for optimisation in noisy environments, SPSA estimates gradients by evaluating the function along random perturbation directions.

SPSA is therefore a suitable candidate for attacking models with non-differentiable components or highly unstable gradient behaviour. These are conditions often encountered in ODE-based or discretised models like the LNN.

Mathematical Representation

Let $x \in \mathbb{R}^d$ be the input and \mathcal{L} the loss function. At each iteration, SPSA perturbs x in a randomly sampled direction $\Delta \sim \{\pm 1\}^d$, and estimates the gradient as:

$$\hat{g}_i = \frac{\mathcal{L}(x + \sigma\Delta) - \mathcal{L}(x - \sigma\Delta)}{2\sigma} \cdot \Delta_i$$

The input is then updated via:

$$x_{t+1}^{\text{adv}} = x_t^{\text{adv}} + \alpha \cdot \text{sign}(\hat{g})$$

Here, σ controls the scale of the finite difference, and α is the step size. The sign function ensures robustness against outliers in the gradient estimate.

Design Choices

In this project, the SPSA attack is implemented using binary random perturbation vectors Δ , that are sampled independently at each iteration. Forward passes are executed twice per iteration to estimate the directional gradient. Once calculated, updates are projected back to an ℓ_∞ ball of radius ϵ around the original input.

```
1 for _ in range(num_iter):
2     delta = torch.randint_like(x, low=0, high=2) * 2 - 1 # + or - 1 vector
3     loss_plus = loss_fn(model(x + sigma * delta), y)
4     loss_minus = loss_fn(model(x - sigma * delta), y)
5     grad_estimate = (loss_plus - loss_minus) / (2 * sigma) * delta
6     x = x + alpha * grad_estimate.sign()
```

Listing 5.4: Simplified SPSA implementation

Reflections on Robustness

- **Gradient-free limitation:** SPSA is powerful when gradients are inaccessible, but its convergence is sensitive to σ and batch size.
- **Hyperparameter sensitivity:** Choosing appropriate α and σ values is important. Small values cause the gradient estimate to vanish and large values cause the model to overshoot the adversarial direction.
- **Noise tolerance:** The LNN’s time-averaged dynamics and implicit smoothness provided resilience against the perturbations introduced by SPSA.

The stochastic nature of this attack mirrors real-world adversarial conditions, where inputs may be corrupted by structured or unstructured noise.

5.6 Time-Warping Attack

Unlike traditional adversarial attacks that modify the magnitude of input features, the time-warping attack alters the temporal structure of the input sequence. This approach is motivated by the fact that many sequence models implicitly assume uniform temporal spacing, and small distortions in timing can have disproportionately large effects on prediction accuracy.

Conceptual Basis

For trajectory prediction, a time-warping attack perturbs the relative spacing between consecutive time steps, modifying the speed (sampling rate) of the underlying system without changing the actual trajectory points themselves. This is effective on models with strong temporal priors, such as recurrent or ODE-based networks.

Mathematical Representation

Let $x = [x_0, x_1, \dots, x_{T-1}]$ be a sequence of length T . A warping function $w : \{0, 1, \dots, T-1\} \rightarrow \mathbb{R}$ maps each time index to a new location. After applying interpolation to enforce fixed-length output, the warped sequence becomes:

$$x_t^{\text{warp}} = x(w(t)), \quad \text{where } w(t) = t + \epsilon \cdot \sin\left(\frac{2\pi t}{T}\right)$$

Here, ϵ determines the amplitude of the distortion. Interpolation (e.g. linear or cubic) is used to ensure that the resulting sequence remains aligned with the original frame size.

Implementation Strategy

The attack is implemented in this project by generating control points across the time domain and applying sinusoidal displacements to simulate acceleration and deceleration patterns. The perturbed sequence is then interpolated back to the original length.

```
1 def warp_sequence(x, epsilon, num_control_points):
2     time = np.linspace(0, 1, len(x))
3     warp = time + epsilon * np.sin(2 * np.pi * time)
4     return interpolate_sequence(x, warp)
```

Listing 5.5: Example Time-Warping Attack Function

Design Choices

The perturbation amplitude (ϵ) is bounded to ensure the warped sequence remained physically plausible and temporally ordered. Linear interpolation is used for stability, since higher-order methods introduce numerical artefacts that empirically degrade learning reproducibility. In addition, the attack is architecture-neutral (since it doesn't require gradient access).

The ability of the continuous-time model (LNN) to handle temporal distortions without significant degradation shows a key advantage. LNNs maintain robustness when underlying assumptions about when those features arrive is attacked.

5.7 Continuous-Time Perturbation Attack

The continuous-time perturbation attack is a novel technique designed specifically for models with internal time dynamics, such as the Liquid Neural Network (LNN). Unlike discrete attacks which perturb input values directly, this method injects structured noise into the temporal dynamics governing the state evolution of the system. This is conceptually aligned with adversarial strategies in control theory and differential equation modelling.

Motivation

In ODE-based models, the output is not solely a function of discrete inputs, but rather of how internal states evolve over time in response to those inputs. Small perturbations to the continuous-time signal (especially during critical integration intervals) can lead to disproportionately large shifts in the terminal state. The attack is designed to evaluate this phenomenon.

Mathematical Representation

Given an input sequence $x(t)$ sampled at discrete steps, and a model defined by the differential equation:

$$\frac{dv}{dt} = F(v, x(t))$$

the adversarial version modifies $x(t)$ into $x^{\text{adv}}(t)$ by injecting structured noise across all integration intervals, effectively perturbing the right-hand side of the ODE during its internal solver steps.

The adversarial input is constructed as:

$$x^{\text{adv}}(t_i) = x(t_i) + \delta_i, \quad \delta_i \sim \mathcal{U}(-\epsilon, \epsilon)$$

where perturbations δ_i are constrained within a norm bound but applied at each ODE unfold step.

Implementation Details

This attack is implemented by modifying the input sequence across all ODE solver substeps inside the `forward` method of the LNN. Unlike standard attacks, which treat input as static, this attack dynamically perturbs the input during internal time integration. The same idea was adapted for discrete models (LSTM, TCN) for comparison, by injecting noise at each time step only once.

```

1  for unfold in range(self.ode_unfolds):
2      perturbed_input = inputs + torch.empty_like(inputs).uniform_(-epsilon,
3                                                     epsilon)
# Proceed with dynamics update using perturbed_input

```

Listing 5.6: Continuous-Time Perturbation Injection

Design Choices

This attack is the only one in the study that targets the solver trajectory itself, not just the input points. For comparability between the LNN and non-ODE models, the same noise patterns were applied to LSTM and TCN (but only once per timestep). For the LNN, they were applied across all ODE unfolds. Uniform noise perturbation shape was used instead of Gaussian to allow strict ℓ_∞ control.

This attack probes the intrinsic robustness of models whose internal computations are sensitive to continuous dynamics. The results illustrate that while the LNN offers meaningful protection at low perturbation levels, it remains vulnerable to adversarial trajectories that disrupt the time integration process itself.

5.8 Summary of Attack Design and Implementation Decisions

This subsection consolidates the key methodological choices made across the six adversarial attacks implemented in this study.

Attack Categories and Coverage

Attack	Gradient Access	Perturbation Type	Temporal Sensitivity
FGSM	White-box	Value-based (single-step)	Low
PGD	White-box	Value-based (multi-step)	Medium
DeepFool-inspired	White-box	Directional / Unbounded	Medium
SPSA	Black-box	Value-based (stochastic)	Medium
Time-Warping	Gradient-free	Time axis distortion	High
Continuous-Time Perturbation	White-box	Internal ODE injection	Very High

Table 5.1: Overview of attack types and model sensitivities.

Implementation Consistency

All attacks adhere to a common evaluation pipeline. The same spiral-based input sequence is used across all models and attacks, and inputs are normalised using the same statistics as during training. Model

outputs are denormalised before computing performance metrics. The perturbation budgets (ϵ) are also standardised across comparable attacks (typically 0.05).

General Attack Design Considerations

- **Reproducibility:** Random seeds are fixed for all stochastic attacks (SPSA, time-warping) to ensure consistent comparison.
- **Numerical Stability:** Small constants ($\delta = 10^{-8}$) are added in division and normalisation steps to prevent undefined behaviour.
- **Model Adaptation:** While some attacks are originally developed for classification or discrete tasks, each was carefully adapted to suit regression-based, sequence-oriented prediction.

5.9 Certified Robustness Analysis of the LNN via Interval Bound Propagation

One of the core contributions of this work is the application of certified robustness techniques to Liquid Neural Networks (LNNs), a model class whose temporal dynamics pose unique challenges to formal analysis. While LNNs have demonstrated strong empirical performance on continuous time-series tasks, their verification under perturbations remains largely unexplored in the literature. In this section, we investigate the provable robustness of the trained LNN using `auto_LiRPA` [20], a state-of-the-art library for neural network bound propagation and formal verification.

Methodology

To assess the model’s stability under input perturbations, we employ *Interval Bound Propagation* (IBP), a forward method which computes tight, conservative bounds on a model’s output when subjected to norm-bounded adversarial noise. Specifically, given a test input x_0 , we define an ℓ_∞ perturbation set $\mathcal{B}_\epsilon(x_0) = \{x : \|x - x_0\|_\infty \leq \epsilon\}$. IBP then propagates the resulting input interval through the model’s layers to produce lower and upper bounds $[\underline{f}(x), \overline{f}(x)]$ on the output across the entire input region.

This approach is particularly suitable for LNNs due to its architectural agnosticism and compatibility with continuous-time formulations, and represents, to the best of our knowledge, the first application of certified bound analysis to a liquid neural model. The experimental results in this section are derived from a single representative input sequence drawn from the validation set.

Certified Output Bounds

Figure 5.1 visualises the certified output interval for dimension 0 of the LNN’s prediction across the temporal horizon. The solid blue curve represents the original output trajectory of the LNN on the unperturbed input, while the shaded region denotes the certified range of possible outputs under all admissible perturbations with $\epsilon = 0.1$. Notably, for the majority of the sequence, the output remains well-contained within the certified bounds, implying that the model’s prediction is provably stable to small variations in the input. However, there is a clear increase in bound looseness in the latter part of the trajectory (timestep 400 onwards), indicating a region of greater uncertainty and higher sensitivity.

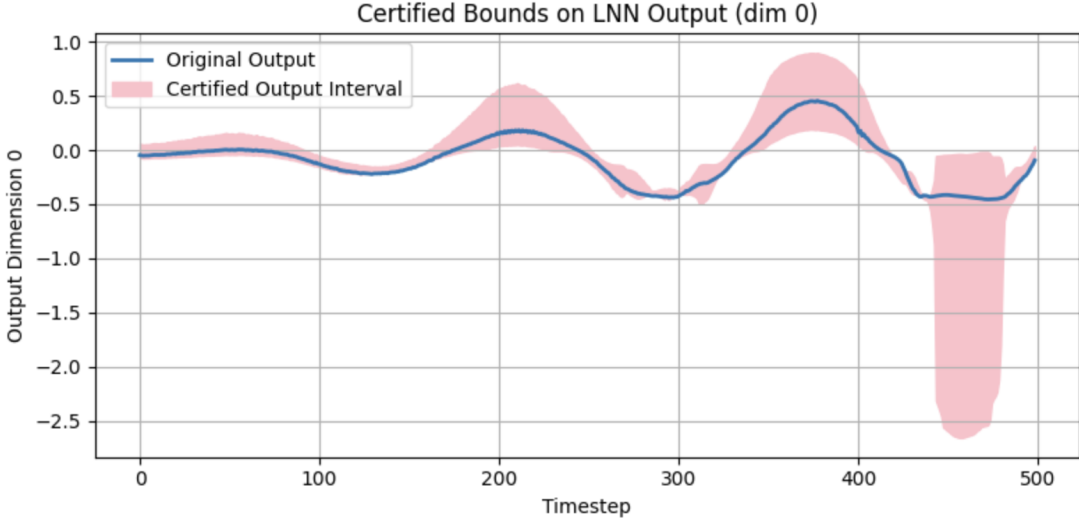


Figure 5.1: Certified output bounds for LNN prediction on dimension 0, computed using IBP via `auto_LiRPA`. The blue line denotes the nominal output; the pink region denotes the certified interval over ℓ_∞ -bounded perturbations.

Bound Width Dynamics

To gain insights into where and when the LNN exhibits greater susceptibility to perturbation, we measure the width of the certified bounds over time. Figure 5.2 presents the bound width (computed as $\bar{f}(x) - f(x)$) separately for each output dimension. The certified intervals vary significantly in both magnitude and temporal structure. In particular, dimension 0 shows sharp spikes in bound width near timesteps 300 and 450, reaching values above 20. These spikes align with regions where the underlying dynamics of the LNN are more nonlinear or where hidden states exhibit rapid transitions.

The bound width in dimension 1, while generally smaller in amplitude, remains elevated throughout the sequence, suggesting a persistent direction of vulnerability in the output space. This observation aligns with adversarial attack results, where perturbations were more effective when targeting dimension 1.

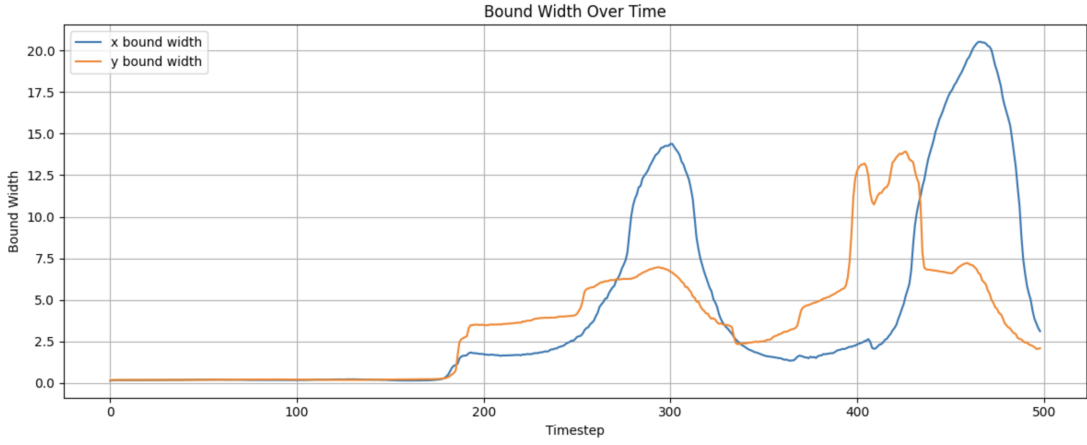


Figure 5.2: Evolution of certified output bound width over time, for both output dimensions of the LNN. Spikes in width correspond to higher uncertainty or sensitivity in the model’s output.

Discussion

These results highlight two key findings. First, the use of IBP enables formal robustness guarantees for LNNs. Second, the certified bounds demonstrate a non-uniform sensitivity profile, with certain regions of the prediction horizon exhibiting high confidence (tight bounds), and others reflecting instability (loose bounds). This fine-grained temporal analysis offers insight into where robustness training or architectural

regularisation may be most effective. Future work could extend this framework using tighter bounds (e.g. CROWN-IBP) or adversarial training to actively reduce the width of certified intervals.

Chapter 6

Evaluation

This chapter covers the quantitative and qualitative evaluation of all four models (LNN, TCN, LSTM, and Transformer) on the same input under various adversarial conditions. We systematically assess how each architecture responds to different types of perturbations, focusing on both performance degradation and qualitative failure modes. These metrics are chosen to capture both the accuracy of trajectory predictions and the model's stability and response to input changes.

6.1 Evaluation Metrics

1. Mean Squared Error (MSE)

The loss function used during training was the Mean Squared Error, given by:

$$\text{MSE} = \frac{1}{T} \sum_{t=1}^T \|\hat{x}_t - x_t\|_2^2$$

where \hat{x}_t is the predicted output at time t , and x_t is the ground truth. MSE measures the average difference between predicted and true trajectories, and is used as a baseline measure of performance under clean (non-adversarial) conditions.

2. Degradation Ratio

To evaluate adversarial impact, the degradation ratio is defined as:

$$\text{Degradation} = \frac{\text{MSE}_{\text{adv}} - \text{MSE}_{\text{clean}}}{\text{MSE}_{\text{clean}} + \delta}$$

where δ is a small constant added to avoid division by zero. This metric captures the relative performance decrease caused by adversarial perturbations. This helps to compare vulnerability across models regardless of their baseline MSE.

3. Deviation Distance

The ℓ_2 deviation between the clean and adversarial predictions is calculated as:

$$\text{Deviation} = \frac{1}{T} \sum_{t=1}^T \|\hat{x}_t^{\text{adv}} - \hat{x}_t^{\text{clean}}\|_2$$

This metric quantifies the visible divergence in predicted trajectories.

Unlike degradation ratio, which depends on the ground truth, this metric focuses purely on how much the model's output changes under perturbation. It is a task-independent measure of functional instability, showing how sensitive the model's outputs are to small adversarial changes.

4. Local Sensitivity (Lipschitz Estimate)

To characterise the smoothness of the model’s function, local sensitivity is estimated by:

$$\text{Sensitivity} = \frac{\|\hat{x}^{\text{adv}} - \hat{x}^{\text{clean}}\|_2}{\|x^{\text{adv}} - x^{\text{clean}}\|_2}$$

This ratio approximates the local Lipschitz constant, capturing how much the output changes in response to small input perturbations. A higher sensitivity indicates that the model has sharp local gradients, potentially making it more brittle. This provides a theoretical metric for robustness, independent of task-specific loss.

6.2 Quantitative Results

Aggregate Metrics Across All Attacks

Model	Avg. Degradation %	Avg. Deviation	Avg. Lipschitz Estimate	Clean MSE
LNN	417.8377	2.1646	0.9441	0.0028
TCN	434.2948	2.2409	1.0071	0.0028
LSTM	287.4266	2.1501	1.0132	0.0044
Transformer	183.5425	2.3060	1.1352	0.0077

Table 6.1: Average robustness metrics across all attacks. Lower values are better for all columns.

Importantly, each model was designed/trained to have comparable MSEs, to allow for fair evaluation.

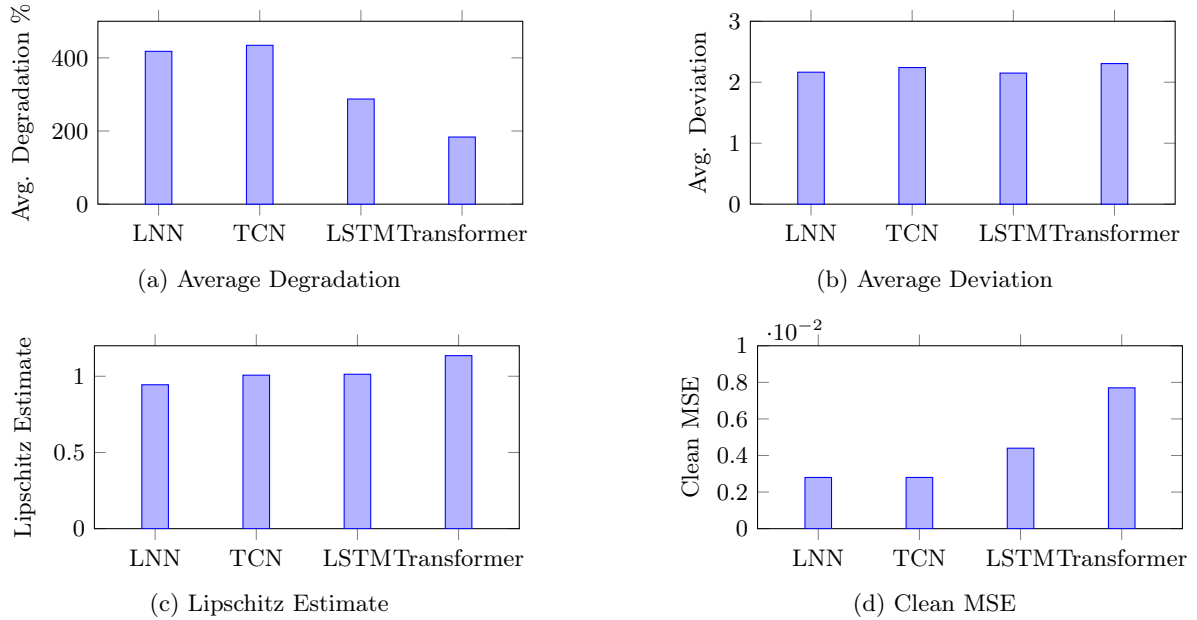


Figure 6.1: Average robustness metrics by model across all attacks. Lower is better.

Attack-Specific Results

The following tables summarise each metric for each model, under various adversarial attacks. Lower values, across all metrics, indicate better robustness.

Attack Type	Degradation (%)			
	LNN	TCN	LSTM	Transformer
FGSM	209.6842	242.5555	169.5259	122.8652
PGD	209.6700	241.7085	169.5408	127.9633
DeepFool-inspired	12.5395	13.9643	11.2735	8.8294
SPSA	36.8717	47.0328	29.7149	21.6053
Time-Warping	1576.5198	1664.5960	1033.6341	579.3263
Continuous-Time Perturb.	458.7058	435.9864	329.8787	242.7071

Table 6.2: Degradation ratios across models for each attack

Attack Type	Deviation			
	LNN	TCN	LSTM	Transformer
FGSM	1.293169	1.419442	1.367006	1.474218
PGD	1.293832	1.416078	1.367387	1.527660
DeepFool-inspired	0.096296	0.101111	0.111709	0.148173
SPSA	0.777944	0.876160	0.842481	0.919706
Time-Warping	6.953865	7.026645	6.882243	7.036172
Continuous-Time Perturb.	2.634408	2.599266	2.601533	2.717356

Table 6.3: Deviation scores across models for each attack

Attack Type	Local Sensitivity (Lipschitz Estimate)			
	LNN	TCN	LSTM	Transformer
FGSM	0.915554	1.004954	0.967830	1.043735
PGD	0.919326	1.005099	0.968100	1.090577
DeepFool-inspired	0.962984	1.011127	1.117503	1.497606
SPSA	0.857096	1.003862	0.964692	1.026772
Time-Warping	0.999767	1.010231	0.989470	1.011601
Continuous-Time Perturb.	1.011938	1.006981	1.005773	1.053375

Table 6.4: Lipschitz Estimate (local sensitivity) across models for each attack

The summary statistics in Table 6.1 and the corresponding bar plots highlight a clear trade-off between clean accuracy and robustness. The Transformer achieves the lowest average degradation (183.54%) and deviation (2.3060), suggesting superior resistance to adversarial attacks overall. However, it also has the highest clean MSE (0.0077) and Lipschitz sensitivity (1.1352), indicating instability under small perturbations and noisier baseline performance. In contrast, the LNN achieves stronger clean performance (0.0028 MSE) and a lower Lipschitz constant (0.9441), but suffers disproportionately under temporal or continuous-time attacks, inflating its degradation average (417.84%). The TCN, while numerically similar to the LNN, is slightly less stable overall, whereas the LSTM maintains balance, with moderate robustness, the lowest average deviation (with the LNN being close), and the second-best clean accuracy. These findings suggest that robustness is not exclusively defined by architectural depth or sequence modelling capability, but instead emerges from the interaction of inductive bias, temporal sensitivity, and perturbation dynamics.

With the lowest average Lipschitz constant (0.9441), the LNN shows the best local sensitivity profile, meaning small changes in input (under L_p norms) cause relatively small changes in output. This is consistent with its ODE-based temporal smoothing.

The LNN is not the most robust across all attacks/metrics, but it does outperform in specific settings, especially against local gradient-based noise. Its architecture offers benefits for tasks involving temporal continuity, but requires careful consideration when deployed in environments with adversarial dynamics that align with its solver steps or temporal assumptions.

6.3 Visual Analysis

While quantitative metrics provide a summary view of model degradation, they can obscure the qualitative character of errors, such as spiralling divergence, phase drift, or geometric distortion. In this section,

we present visual comparisons between clean and adversarial predictions to better understand how each model's internal representation and output trajectory is disrupted.

Visualisation Methodology

For each attack and model combination, clean and adversarial predictions were overlaid on the same plot. Ground truth trajectories were shown for reference, and all sequences were denormalised prior to plotting.

Each figure highlights a specific failure mode characteristic to the architecture under consideration.

FGSM Attack Results

The FGSM attack was applied to all three models under a fixed perturbation budget $\epsilon = 0.05$.

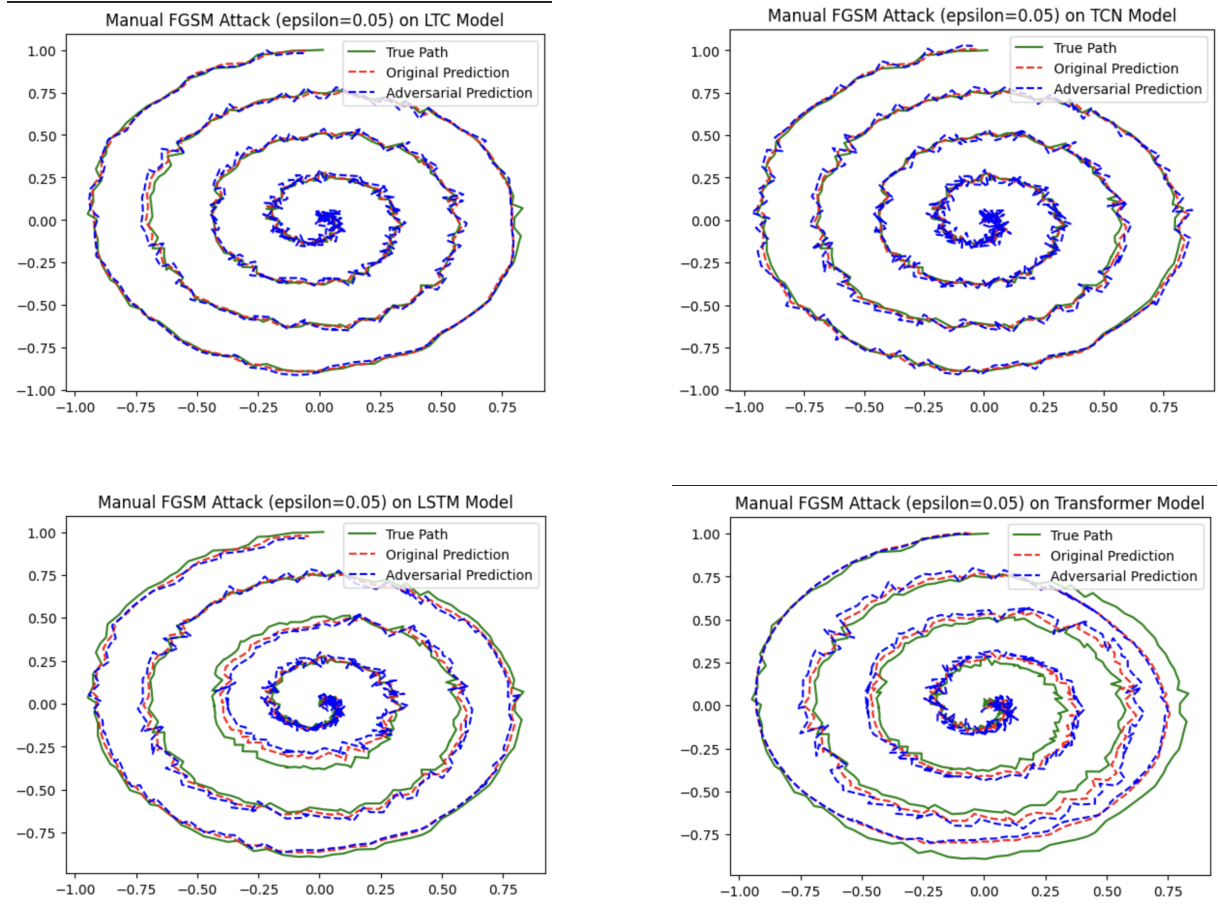


Figure 6.2: Predicted, Target, and Adversarial projections under FGSM attack on LTC, TCN, LSTM and Transformer models. Using the same denormalised input spiral.

From figure 6.2, the Liquid Neural Network (LTC) shows notable resilience, maintaining close alignment between its original and adversarial predictions for the majority of the trajectory. While minor deviations are visible, especially near the inner spiral, the global structure remains coherent. This is likely due to the continuous-time membrane integration and temporal smoothing induced by the ODE solver.

In contrast, the TCN and Transformer models show pronounced adversarial distortion. The TCN suffers from its lack of recurrent memory, leading to sharp deflections in regions of local perturbation.

The Transformer, despite its capacity, exhibits highly unstable predictions under attack, likely due to its limited inductive bias and sensitivity to global input shifts.

The LSTM model shows intermediate robustness: although its gating structure filters out some perturbations, it remains vulnerable to gradient-based attacks that propagate through long-term memory.

Thus, the LTC’s continuous dynamics and biophysical parameterisation seem to have stabilising effect, outperforming the more discrete or attention-based baselines under single-step adversarial pressure.

PGD Attack Results

PGD, as a stronger attack method, caused greater degradation than FGSM across all models, with stronger effect on deeper temporal structures.

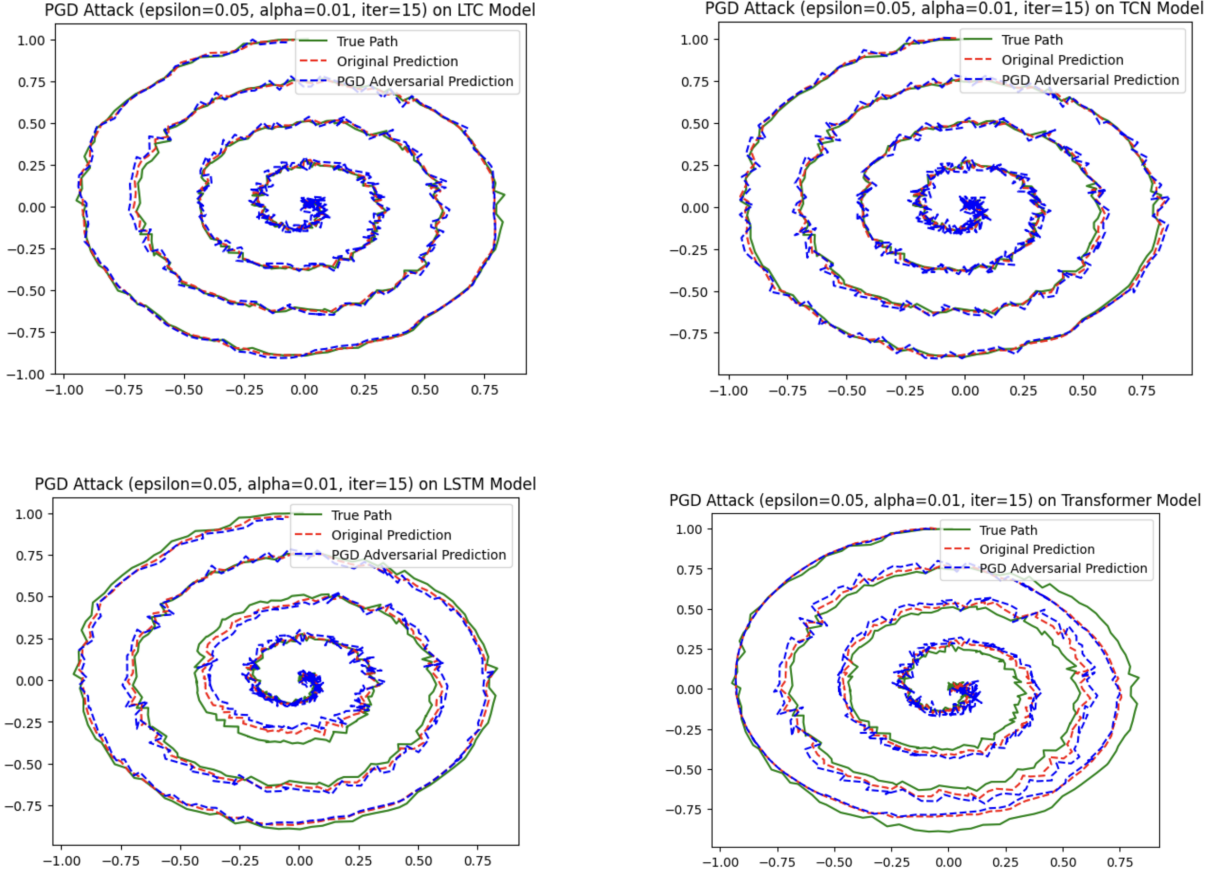


Figure 6.3: Predicted, Target, and Adversarial projections under PGD attack on LTC, TCN, LSTM and Transformer models. Using the same denormalised input spiral.

Figure 6.3 presents the effect of a 15-step PGD attack on each model, using $\epsilon = 0.05$ and $\alpha = 0.01$. The LTC continues to exhibit strong robustness, with its adversarial trajectory (blue) closely shadowing the original prediction (red) and the true path (green). Despite minor divergence being visible (particularly near the spiral’s centre where curvature is high) the global structure remains largely preserved. This resilience is again due to the regularising effect of continuous-time dynamics and the internal ODE solver. For the PGD attack, this limits perturbations across integration steps, dampening the cumulative effect.

In contrast, the Transformer model suffers substantial degradation. Its adversarial trajectory spirals off course significantly, as a result of the model’s sensitivity to small input shifts and lack of temporal inductive bias.

The LSTM also displays clear distortion, particularly in early spiral turns, reflecting how perturbations to the input cascade through long-range memory states.

The TCN, while affected, shows slightly improved robustness relative to the Transformer and LSTM, likely due to the inherent smoothing effect of its dilated convolutions. The absence of state memory however limits its ability to resist cumulative perturbation.

The LTC model still seems to stabilise predictions under iterative, gradient-based adversaries like PGD.

Deepfool-Like Attack Results

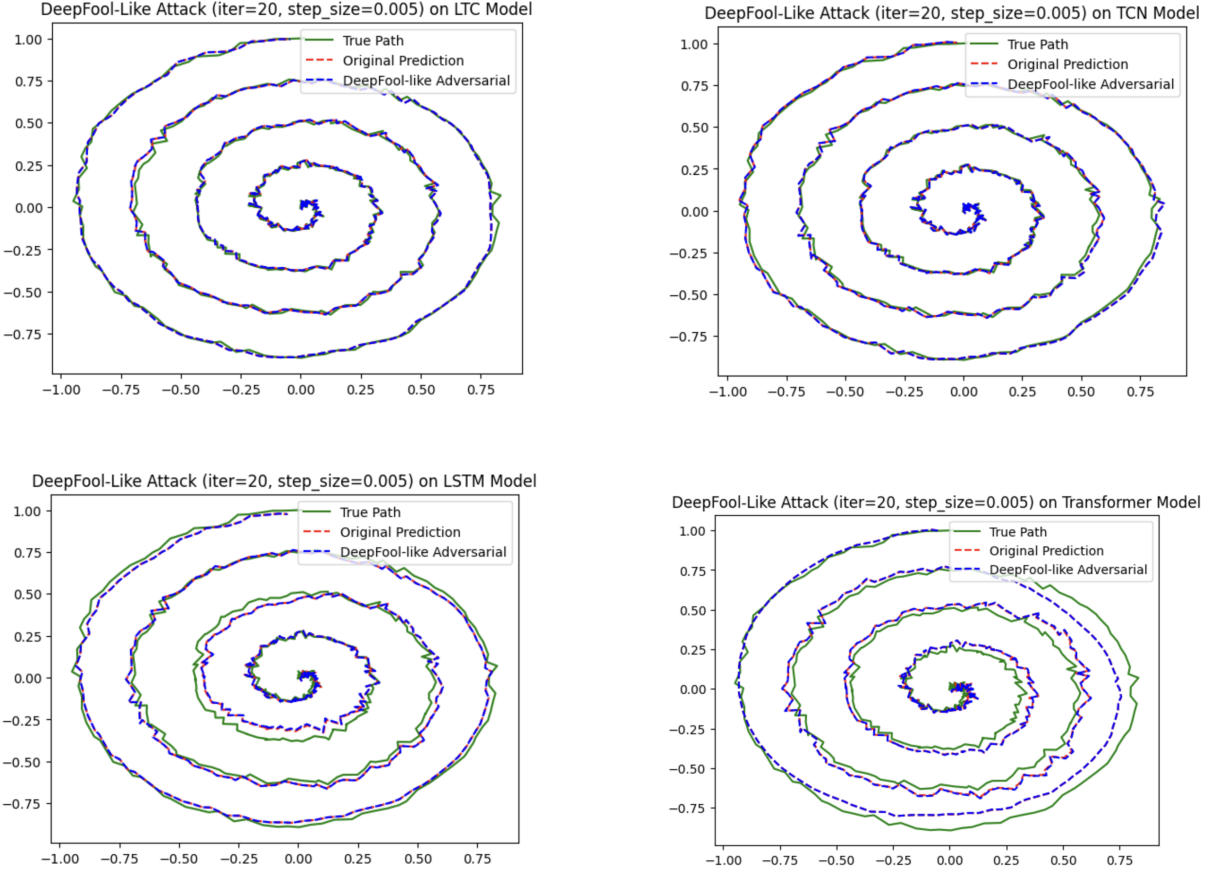


Figure 6.4: Predicted, Target, and Adversarial projections under Deepfool-Like attack on LTC, TCN, LSTM and Transformer models. Using the same denormalised input spiral.

The plots in Figure 6.4 show the effects of a DeepFool-like iterative attack (20 steps, step size = 0.005) adapted for regression. Unlike PGD or FGSM, which aim for maximal distortion within a norm-bound, DeepFool attempts to perturb inputs just enough to cross decision boundaries. In this case, this corresponds to inducing maximal deviation in continuous predictions. The Transformer model shows the highest vulnerability: its adversarial trajectory (blue) diverges significantly from the true path (green), especially in the inner spiral turns where minor distortions amplify rapidly.

The LSTM is similarly affected, to a slightly lesser extent, with perturbations distorting predictions in both early and late sequence segments. This aligns with known vulnerability of memory-based architectures to accumulated gradient signals across time.

The TCN demonstrates moderate resilience. While some deviations occur, especially near tight curvatures, the global shape is retained.

The LTC model remains the most stable under this attack. Its adversarial predictions are closer to the original (red), indicating that the internal ODE dynamics of the LNN may diffuse perturbations temporally, flattening adversarial gradients.

SPSA Results

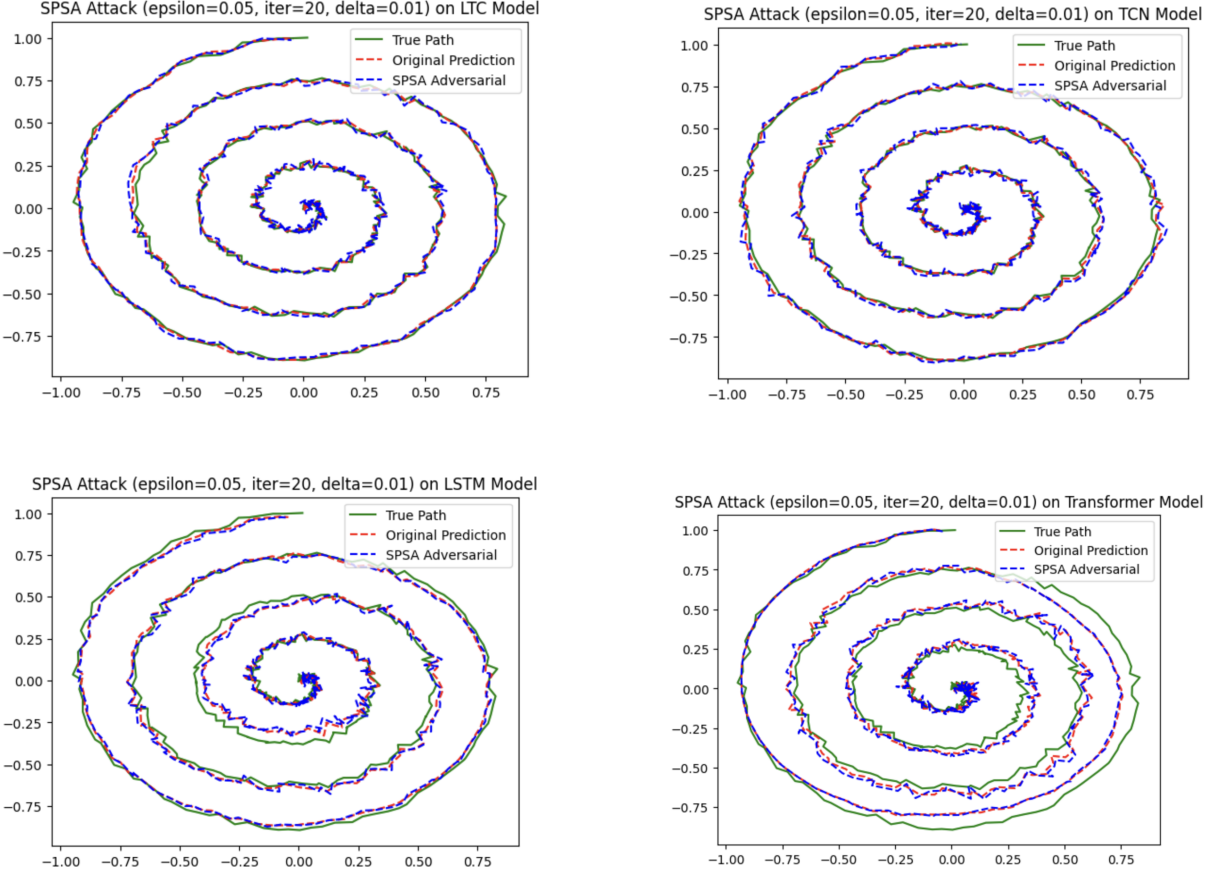


Figure 6.5: Predicted, Target, and Adversarial projections under SPSA attack on LTC, TCN, LSTM and Transformer models. Using the same denormalised input spiral.

As shown in Figure 6.5, the impact of SPSA is comparatively mild across all models, consistent with its tendency to explore less optimal perturbation directions relative to gradient-based attacks like PGD. It does still reveal architectural differences in robustness.

The LTC model shows minimal divergence under SPSA, maintaining tight alignment between original and adversarial predictions. This further reinforces it's resilience observed in prior attack scenarios.

The TCN and Transformer show more visible degradation in the spiral's outer loops, indicating that their fixed receptive fields and positional encoding mechanisms are more easily disrupted by uniform input noise.

The LSTM shows moderate vulnerability, with adversarial traces deviating steadily from the true trajectory over time.

Time Warping Attack Results

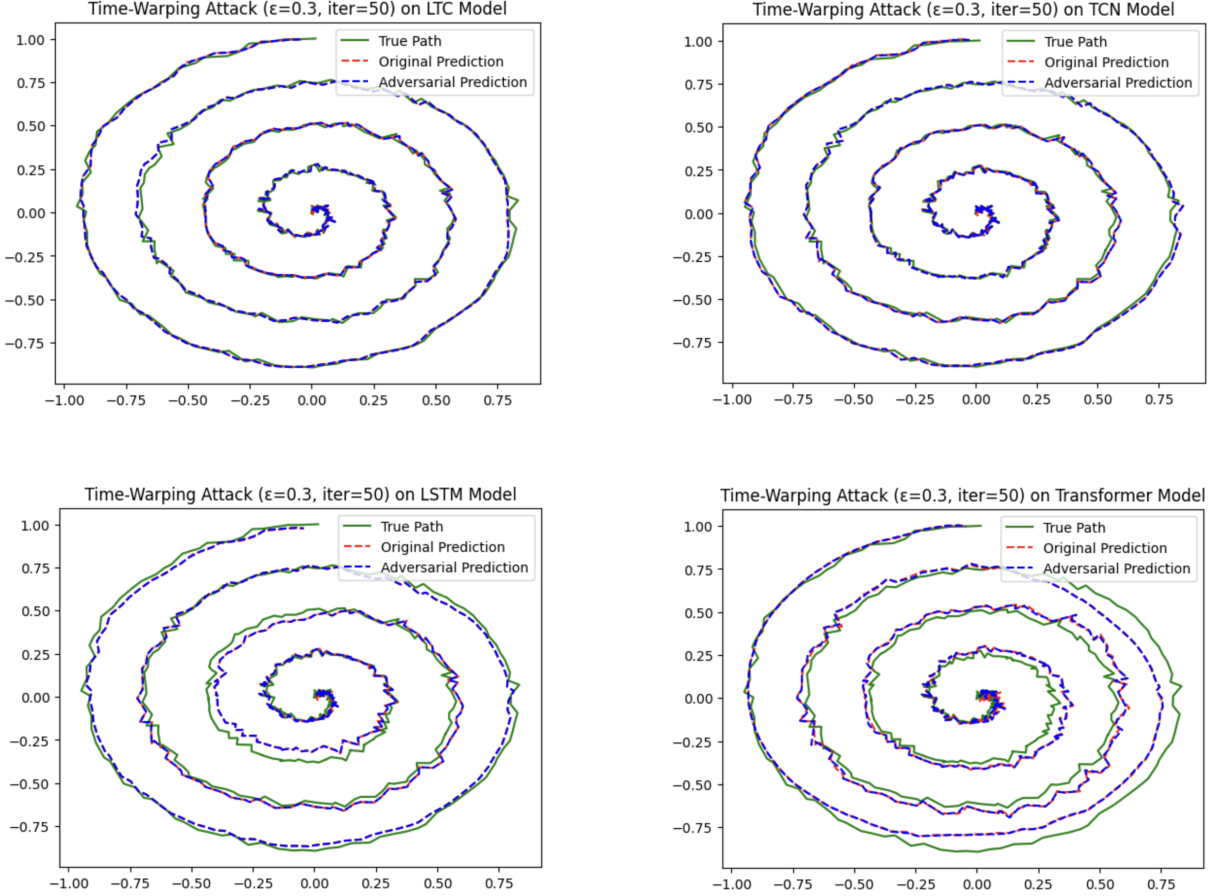


Figure 6.6: Predicted, Target, and Adversarial projections under Time Warping attack on LTC, TCN, LSTM and Transformer models. Using the same denormalised input spiral.

Figure 6.6 displays the impact of a time-warping attack on each model. This attack perturbs the temporal spacing of input points without altering the values themselves, distorting the perceived dynamics of the sequence. The LSTM model appears particularly sensitive, with adversarial predictions deviating noticeably from the true path green, especially in outer spiral turns. This is expected given the LSTM's reliance on a fixed temporal memory structure, which is easily disrupted by misaligned temporal cues.

Similarly, the Transformer struggles to adapt to the warped temporal signal, showing severe prediction drift. This is due to its reliance on position encodings that assume uniform spacing.

In contrast, the TCN maintains good alignment with the true path, showing resilience due to its convolutional structure and dilated receptive fields, which provide a form of local smoothing.

The Liquid Neural Network (LTC) performs best under this attack. Its continuous-time dynamics and internal state integration appear to absorb the warping, maintaining alignment between the adversarial and original predictions. This reinforces the hypothesis that ODE-based temporal models like LNNs are inherently more invariant to temporal distortions, making them better suited for tasks with irregular or corrupted time sampling.

Continuous-Time Adversarial Perturbation Attack Results

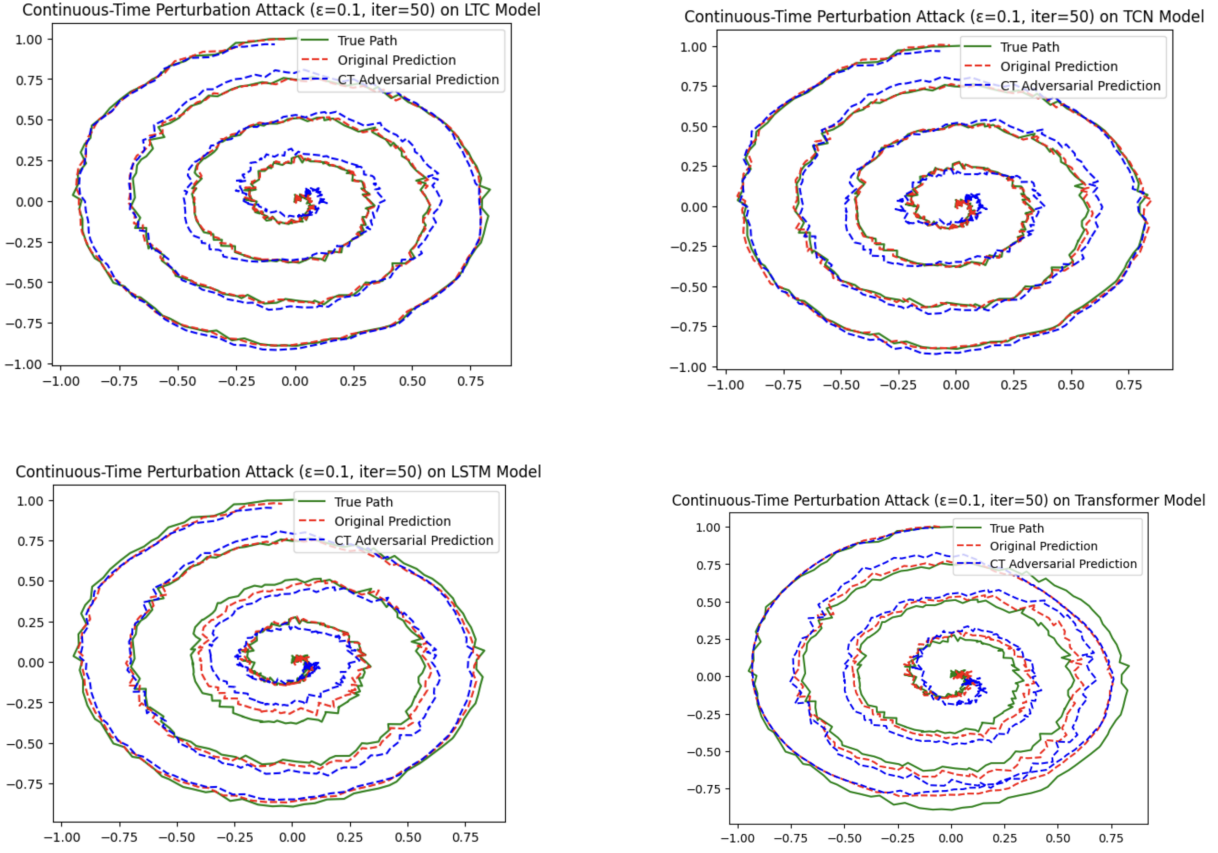


Figure 6.7: Predicted, Target, and Adversarial projections under Continuous-Time Adversarial Perturbation attack on LTC, TCN, LSTM and Transformer models. Using the same denormalised input spiral.

The continuous-time perturbation attack, specifically tailored for models governed by differential equations, targets the latent state evolution rather than directly modifying the input trajectory. This makes it particularly suited for evaluating the Liquid Neural Network (LTC), whose continuous-time membrane dynamics offer both flexibility and potential vulnerability to such perturbations.

As shown in Figure 6.7, the LTC model remains relatively stable under attack, with adversarial predictions closely tracking the original predictions throughout the spiral. This indicates that the internal ODE dynamics, when properly regularised, can absorb structured noise and maintain functional predictions.

The TCN and LSTM models however exhibit more pronounced deviations, especially in the outer spiral turns, suggesting that perturbations which indirectly affect temporal relationships (e.g. via integration-like behaviour) are disruptive to their sequential representations.

The Transformer, which lacks an explicit temporal evolution mechanism, is highly vulnerable to these perturbations, with the adversarial trajectory diverging significantly from the true path.

This again highlights a key advantage of biologically inspired continuous-time models (LNNs) in handling dynamic, structured adversarial noise.

Interpretation

Models with rigid temporal assumptions or recurrent memory (LSTM) are more susceptible to both magnitude and timing distortions, whereas continuous-time dynamics (LNN) offer meaningful resistance. However, no model was universally robust, and each architecture exhibited specific weaknesses when faced with particular perturbation types.

6.4 Discussion of Results

Architecture-Specific Vulnerabilities

A cross-attack comparison reveals that each model exhibits distinct vulnerabilities determined by its inductive biases. The LSTM is particularly sensitive to early-sequence perturbations due to its recurrent memory, leading to long-range compounding errors. TCNs, while able to contain noise locally, struggle to restore global structure after distortion. The Transformer’s self-attention allows some recovery via context redistribution, but it remains susceptible to phase collapse under structured attacks (when key tokens are disrupted). The Liquid Neural Network (LNN), by contrast, preserves smoothness but responds poorly to high-frequency or temporally persistent adversaries, as shown in its high degradation under continuous-time and PGD perturbations.

Model Design

These results align with the models’ architectural design. LSTMs encode state recursively, which amplifies small errors. TCNs filter over fixed windows, making them blind to long-term disruptions. Transformers rely on positional encoding without state memory, making them sensitive to ordering distortions. LNNs model time explicitly via ODEs, offering natural resistance to time-warping and continuity-based attacks, but remain dependent on solver stability and hyperparameter tuning.

Temporal Drift and Geometric Collapse

A consistent phenomenon observed in PGD, DeepFool-like, and continuous-time attacks is phase drift. This is where adversarial trajectories spiral inward or outward over time. This error accumulates directionally rather than randomly, reflecting the effectiveness of gradient-aligned perturbations in destabilising long-term dynamics.

Attacks like FGSM and SPSA however result in less coherent but more transient distortions, typically recoverable unless they coincide with critical points in the trajectory.

6.5 Defences for Liquid Neural Networks

There are a range of theoretical strategies that can be used to mitigate adversarial vulnerability in Liquid Neural Networks (LNNs), with comparisons to TCN and LSTM where relevant.

Adversarial Training and Perturbation Smoothing

While adversarial training has been shown effective in conventional networks [8], its adaptation to continuous-time models like LNNs requires careful consideration. One potential direction is continuous-time adversarial training, where adversarial perturbations are applied not only at the input level but across intermediate ODE solver steps. This would simulate realistic, dynamic threats such as time-warping or sensor noise.

In addition, input noise injection (e.g. Gaussian or uniform noise) could promote smoother input-output mappings, as seen in denoising autoencoders [21]. For LNNs, perturbing the input current $u_i(t)$ over time can improve resistance to minor temporal distortions.

Structural Regularisation in Liquid Architectures

A core advantage of LNNs lies in their biologically-inspired dynamics:

$$\frac{dv_i}{dt} = -\frac{v_i}{\tau} + \sum_j W_{ij} \cdot \sigma(v_j(t)) + u_i(t) \quad (6.1)$$

Here, the decay constant τ and activation function σ are learnable. Imposing soft constraints on τ or bounding the membrane potential v_i could prevent exponential state divergence under perturbation.

Figure 6.8 illustrates how limiting the slope of the state curve over time may preserve stability.

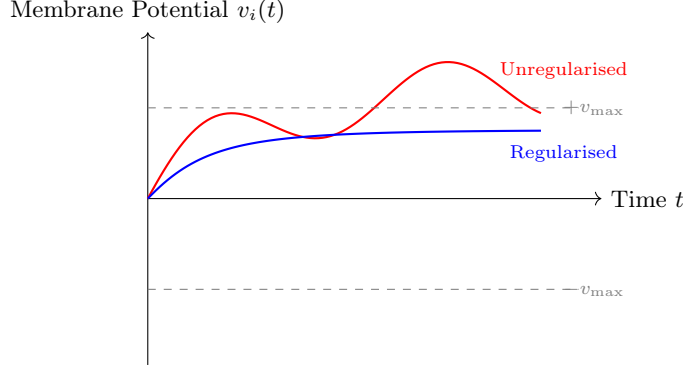


Figure 6.8: LNN membrane potential evolution with and without regularisation. Regularisation limits state drift, improving stability under input perturbations.

Additionally, dynamically adjusting the solver step size during inference (based on detected input smoothness or gradient norms) can act as another form of defence. Such adaptive schemes are supported by work in neural ODE robustness [22, 23].

Temporal Input Filtering and Quantisation

Preprocessing defences offer architecture-agnostic robustness benefits. Applying a low-pass filter to the input trajectory, defined as:

$$x_t^{\text{filtered}} = \alpha x_t + (1 - \alpha)x_{t-1}, \quad \alpha \in [0, 1] \quad (6.2)$$

can suppress high-frequency adversarial noise typical in gradient-based attacks.

Similarly, discretising the time component or input position encoding:

$$\text{quantised}_t = \left\lfloor \frac{t}{\Delta t} \right\rfloor \quad (6.3)$$

has been hypothesised to improve invariance to small timing shifts [24].

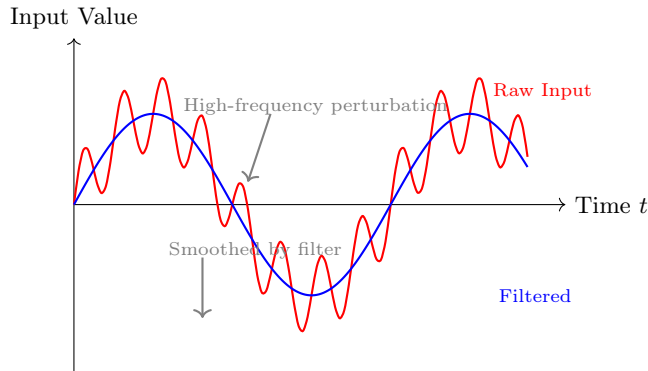


Figure 6.9: Illustration of low-pass temporal filtering as a defence mechanism. Sharp perturbations are smoothed before reaching the model.

Inductive Bias and Solver-Aware Stability

Unlike discrete models, LNNs require the solver to faithfully capture non-linear temporal dynamics. This opens unique defence opportunities:

- **Step-size modulation:** Smaller solver steps reduce numerical error accumulation under perturbed inputs.
- **Activation bounding:** Enforcing $|v_i(t)| \leq V_{\max}$ could prevent state explosion.

- **Implicit regularisation:** Using solver-aware loss terms penalising high curvature over time.

These mechanisms can be integrated during training to enforce smooth, stable behaviour even when inputs deviate adversarially.

Limitations

Liquid models do also present unique challenges, since adversarial attacks in continuous time are underexplored and difficult to formalise. Solver regularisation may reduce model expressivity or increase compute cost. There is also a risk that filtering can remove meaningful signal patterns in real-world tasks.

Practically incorporating formal verification [25] or hybrid models that mix discrete and continuous pathways may further improve LNN reliability.

Chapter 7

Conclusion

7.1 Summary of Work

This project set out to conduct a comprehensive investigation into the adversarial robustness of Liquid Neural Networks (LNNs) compared to more established architectures, including LSTMs, Temporal Convolutional Networks (TCNs), and Transformers, under a variety of attack conditions. A key objective was to evaluate whether the biologically inspired dynamics and continuous-time formulation of LNNs confer practical advantages in the face of adversarial perturbations, especially on complex, low-data temporal tasks.

A full suite of adversarial attacks was implemented, spanning both white-box (FGSM, PGD, DeepFool-inspired) and black-box (SPSA) settings, along with novel time-based strategies (time-warping and continuous-time perturbation). Each attack was evaluated on its effectiveness against the trajectory prediction capabilities of each model. Performance metrics such as degradation, deviation, and local Lipschitz estimates were recorded and analysed both quantitatively and visually. This multi-perspective analysis allowed for the identification of distinct architectural vulnerabilities, including phase drift in LSTMs, local distortion in TCNs, and solver-instability in LNNs.

In addition to empirical attacks, a robustness certification component was included using the `auto_LiRPA` framework. This formal analysis provided lower bounds on model behaviour under norm-bounded perturbations, offering a complementary perspective to empirical evaluation. For LNNs in particular, the ability to propagate bounds through nonlinear ODE solvers revealed both strengths and gaps in their stability guarantees.

These findings carry important implications for deployment of LNNs:

- When deploying models in adversarial or uncertain environments, the temporal assumptions of the architecture must be scrutinised.
- Robustness is context-dependent — no model is universally secure, and the choice of architecture should be informed by the anticipated type of input perturbation.
- LNNs offer promising directions for tasks where input timing is noisy or attacker-controlled, such as sensor-based monitoring or robotics.

Throughout the report, care was taken to contextualise results with architectural insights, avoiding overreliance on scalar metrics and drawing attention to trajectory-level failure modes. The novelty of applying such a wide array of adversarial techniques—many of which had never been adapted to LNNs—underscores the originality of this work. Where prior literature focused on vision or classification tasks, this report contributes to the limited body of research evaluating adversarial robustness in continuous-time sequence prediction.

7.2 Future Work

Several promising directions for future research have emerged. First, the integration of robustness training techniques such as adversarial training, certified training, or interval-based regularisation could be

explored for LNNs to further enhance their defensive capabilities. Given their continuous-time nature, LNNs may benefit from training procedures that regularise not only model weights but also the trajectories induced by adversarial schedules.

Second, while this project focused on 2D synthetic spirals to maintain interpretability, real-world time series datasets—such as physiological signals or control system traces—would provide a stronger testbed for evaluating robustness in practical scenarios. Extending the current framework to handle larger, higher-dimensional datasets with irregular sampling would be a valuable contribution.

Third, the certification methods used here rely on interval and bound propagation through neural ODE solvers. However, more recent methods such as zonotope or Taylor-based reachability analysis could improve the tightness of certified bounds. Likewise, further analysis of solver dynamics—especially in stiff or underdamped regimes—may yield deeper understanding of how adversarial signals interact with time-discretisation schemes.

Finally, the Transformer model’s relatively poor performance under perturbation raises important questions about its inductive biases in temporal tasks. Investigating hybrid models, such as Liquid Transformers or ODE-infused attention layers, could bridge the gap between high-capacity architectures and biologically plausible time modelling.

Taken together, the findings of this project confirm that LNNs offer a promising and underexplored direction for adversarially robust temporal modelling. While not immune to attack, their continuous-time formulation introduces useful inductive properties that—when properly harnessed—may offer both practical and theoretical benefits for future AI systems.

Bibliography

- [1] Hasani R, Lechner M, Amini A, Rus D, Grosu R. Liquid Time-Constant Networks. Proceedings of the AAAI Conference on Artificial Intelligence. 2021 May;35(9):7657-66. Available from: <https://ojs.aaai.org/index.php/AAAI/article/view/16936>.
- [2] Frank E, Fekri F. Learning Neuron Dynamics: The Age of SPIKING 2.0. arXiv preprint arXiv:240720590. 2024. Available from: <https://arxiv.org/abs/2407.20590>.
- [3] TEDx Talks. Liquid Neural Networks | Ramin Hasani | TEDxMIT; 2023. Accessed 2025-01-20. https://www.ted.com/talks/ramin_hasani_liquid_neural_networks.
- [4] Chahine M, Hasani R, Kao P, Ray A, Shubert R, Lechner M, et al. Robust Flight Navigation Out of Distribution with Liquid Neural Networks. Science Robotics. 2023 Apr;8(77):eadc8892. Available from: <https://www.science.org/doi/10.1126/scirobotics.adc8892>.
- [5] Szegedy C, Zaremba W, Sutskever I, Bruna J, Erhan D, Goodfellow I, et al. Intriguing properties of neural networks. arXiv preprint arXiv:13126199. 2013.
- [6] Goodfellow IJ, Shlens J, Szegedy C. Explaining and harnessing adversarial examples. arXiv preprint arXiv:14126572. 2014.
- [7] Hasani R, Lechner M, Amini A, Rus D, Grosu R. Liquid Time-Constant Networks. In: Proceedings of the 34th International Conference on Neural Information Processing (ICONIP). vol. 12533 of Lecture Notes in Computer Science. Springer; 2020. p. 650-61.
- [8] Madry A, Makelov A, Schmidt L, Tsipras D, Vladu A. Towards Deep Learning Models Resistant to Adversarial Attacks. In: International Conference on Learning Representations (ICLR); 2018. Available from: <https://openreview.net/forum?id=rJzIBfZAb>.
- [9] Moosavi-Dezfooli SM, Fawzi A, Frossard P. DeepFool: a simple and accurate method to fool deep neural networks. In: Proceedings of the IEEE conference on computer vision and pattern recognition; 2016. p. 2574-82.
- [10] Uesato J, O'Donoghue B, van den Oord A, Kohli P. Adversarial risk and the dangers of evaluating against weak attacks. International Conference on Machine Learning (ICML). 2018.
- [11] Cisse M, Adi Y, Neverova N, Keshet J. Houdini: Fooling deep structured prediction models. In: Advances in Neural Information Processing Systems; 2017. p. 6977-87.
- [12] Sun C, Shrivastava A, Singh S, Gupta A. Natural and adversarial error detection using invariant predictors. In: International Conference on Machine Learning (ICML); 2018. .
- [13] Weng TW, Zhang H, Chen PY, Yi J, Su D, Gao Y, et al. Evaluating the robustness of neural networks: An extreme value theory approach. In: International Conference on Learning Representations (ICLR); 2018. .
- [14] Dong X, Yao S, Hu H, Wang Y, Li S, Zhang Z, et al. Benchmarking Robustness of Neural Networks on Time-Series Data. arXiv preprint arXiv:200312298. 2020.
- [15] Henriksen P, Lomuscio A. Efficient Neural Network Verification via Adaptive Refinement and Adversarial Search. In: Proceedings of the 24th International Conference on Tools and Algorithms for the Construction and Analysis of Systems (TACAS). Springer; 2024. To appear.
- [16] Zhang H, Weng TW, Chen PY, Hsieh CJ, Daniel L. Efficient Neural Network Robustness Certification with General Activation Functions. arXiv; 2018.

- [17] Hermann M, Bellec G. LTCtutorial: Liquid Time-Constant Neural Networks; 2022. GitHub repository, accessed: 2025-06-13. <https://github.com/KPEKEP/LTCtutorial>.
- [18] Vaswani A, Shazeer N, Parmar N, Uszkoreit J, Jones L, Gomez AN, et al. Attention Is All You Need. In: Proceedings of the 31st International Conference on Neural Information Processing Systems (NeurIPS). Curran Associates, Inc.; 2017. Available from: https://proceedings.neurips.cc/paper_files/paper/2017/file/3f5ee243547dee91fb053c1c4a845aa-Paper.pdf.
- [19] Goodfellow IJ, Shlens J, Szegedy C. Explaining and Harnessing Adversarial Examples. arXiv preprint. 2015;arXiv:1412.6572. Available from: <https://arxiv.org/abs/1412.6572>.
- [20] Wang Z, Zhang H, Weng TW, Daniel L, Hsieh CJ. auto_LiRPA: A Library for Certified Robustness in PyTorch; 2022. Accessed: 2025-06-13. https://github.com/Verified-Intelligence/auto_LiRPA.
- [21] Vincent P, Larochelle H, Bengio Y, Manzagol PA. Extracting and composing robust features with denoising autoencoders. In: Proceedings of the 25th international conference on Machine learning. ACM; 2008. p. 1096-103.
- [22] Dupont E, Doucet A, Teh YW. Augmented neural ODEs. Advances in Neural Information Processing Systems. 2019;32.
- [23] Finlay C, Papamakarios G. Trainable verification of neural networks. Advances in Neural Information Processing Systems. 2020;33:11427-38.
- [24] Wang Y, Ma X, Bailey J, Zisselman E, Ye J, Liu B, et al. Adversarial defense by restricting the hidden space of deep neural networks. In: European Conference on Computer Vision (ECCV). Springer; 2018. p. 350-66.
- [25] Zhang L, Zhang K, Zhang K, Weng TW. Towards certifying LSTM robustness to adversarial perturbations. IEEE Transactions on Information Forensics and Security. 2022;17:439-54.

Declaration

Use of Generative AI

I acknowledge the use of GPT-4o (OpenAI, <https://chat.openai.com/>) to design the report structure, to convert pre-existing diagrams to latex diagrams, and to assist with finding research papers. I confirm that no content generated by AI has been presented as my own work.

Ethical Considerations

This project is a software-based initiative and does not involve experiments on any living beings. Additionally, it poses no significant physical or environmental safety risks. No personal or sensitive data is collected or utilized during the course of this work. All datasets used for experimental purposes will be sourced from publicly available open-source repositories. In addition, care will be taken to ensure all datasets are appropriately anonymised and used in compliance with relevant data protection regulations.

There are no immediate military/high-risk applications envisioned for this project. However, liquid neural networks are highly adaptable and capable of handling complex, dynamic tasks. Thus, they could be misused in fields such as surveillance, privacy-invasive technologies, and military systems. Developing robust verification methods would increase the reliability of LNNs, which carries the risk of increasing their impact in such areas. However, since this is a theoretical verification project, this risk is no greater than that of other general-purpose machine learning research.

Ensuring that the verification process is transparent, reproducible, and understandable is important. If verification methods become too opaque, it could create barriers to accountability and limit their ethical deployment.

Software development for this project may require use of open-source libraries. Where relevant, credit will be given to authors. The appropriate academic license will be obtained if any proprietary software is needed for development/experimentation. Proprietary software will not be distributed in the final framework produced.

Sustainability

To minimise environmental impact, all experiments were conducted on DoC GPU clusters with batch processing to minimise energy usage. Hyperparameter searches and model training were kept computationally efficient through early stopping and low-complexity model variants, reducing unnecessary compute cycles.

Data and Materials

The source code repository can be found here: <https://github.com/ViyanR/LTCFYP>.